Supplementary Information

July 28, 2021

Contents

List of Figures

Supplementary Note 1: Correlation of PC betas across sex groups

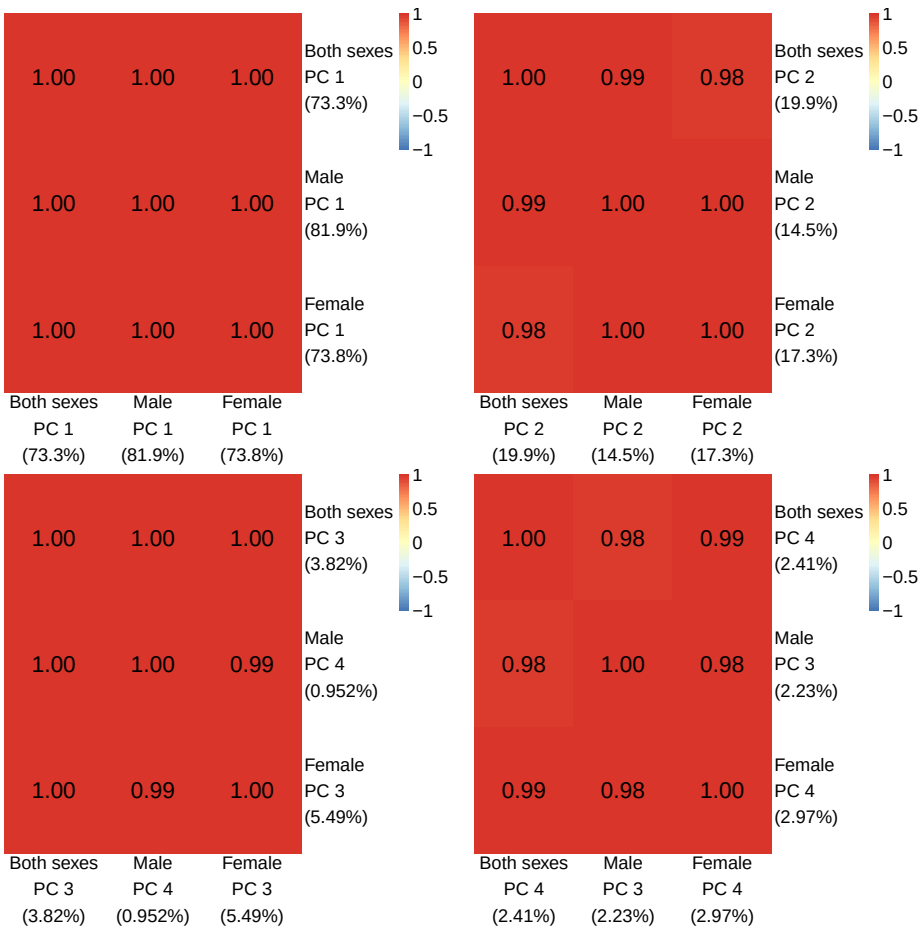

Supplementary figure 1: Correlation of PC effect estimates obtained using PC loadings from different sex groups. The SNP effects for the anthropometric traits were estimated in the combined sex group, from which their effects on the top four PCs were calculated using the loadings from each of the three sex groups, i.e. both sexes combined, men, and women. The correlation was calculated across SNPs which were selected in the combined sex group.

Supplementary Note 2: Correlation of PC betas with different traits

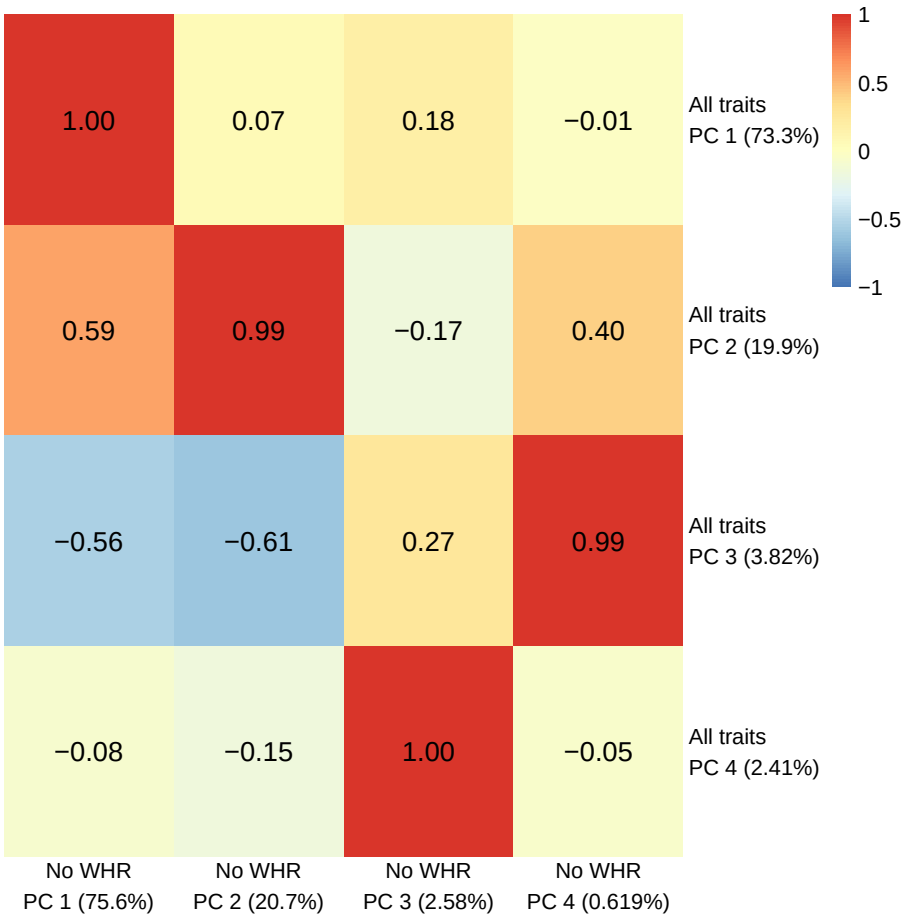

Supplementary figure 2: Correlation of PC effect estimates obtained using PC loadings from all 14 anthropometric traits or without height or waist-to-hip ratio (WHR). The SNP effects for the anthropometric traits were estimated in the combined sex group, from which their effects on the top four PCs were calculated. The correlation was calculated across SNPs which were selected in the PCs using all traits (thereby providing more SNPs).

Supplementary Note 3: Phenotypic correlation

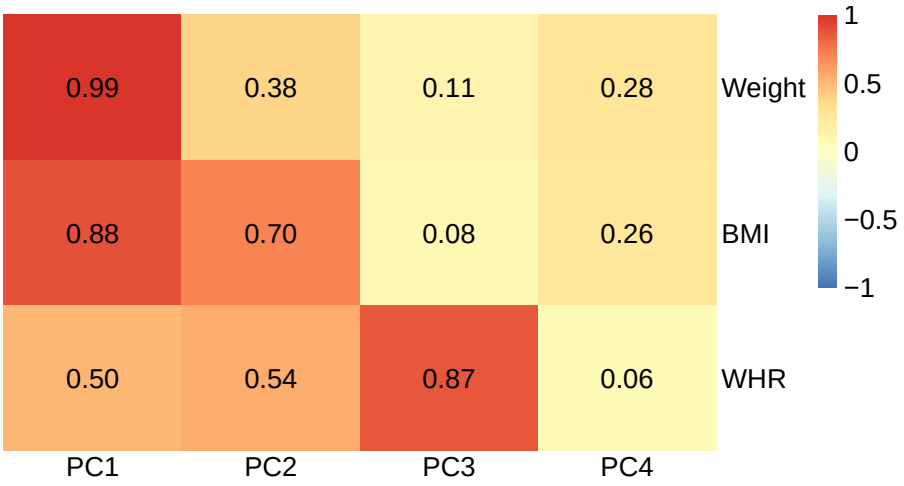

Supplementary figure 3: Phenotypic correlation between PCs and common measures of obesity. The phenotypic PCs were obtained by applying the genetic PC loadings to the anthropometric traits in a subset of 371,529 unrelated white individuals in the UK Biobank. The full matrix of phenotypic correlations is available in Supplementary Table 11.

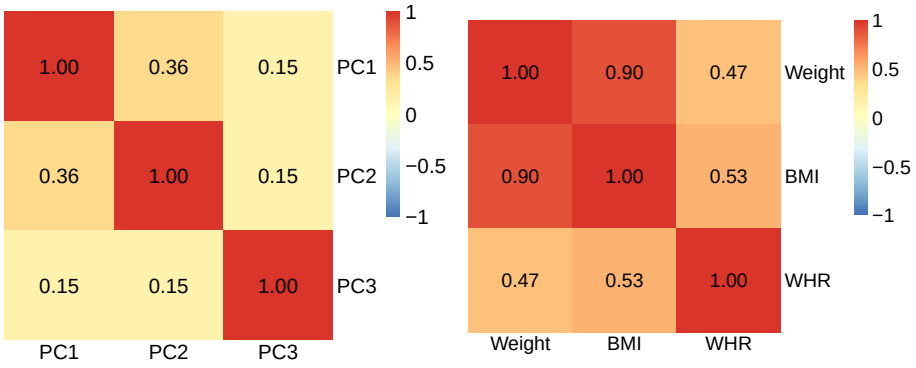

(a) Phenotypic correlation of PCs

(b) Phenotypic correlation of traits

Supplementary figure 4: Comparison of the phenotypic correlation of PCs and the individual traits most similar to each. The phenotypic PCs were obtained by applying the genetic PC loadings to the anthropometric traits in a subset of 371,529 unrelated white individuals in the UK Biobank. The full matrix of phenotypic correlations is available in the Supplementary Table 11.

Supplementary Note 4: Comparison of exposure effects using cross-sex IVW MR

4.1 Effects on diseases

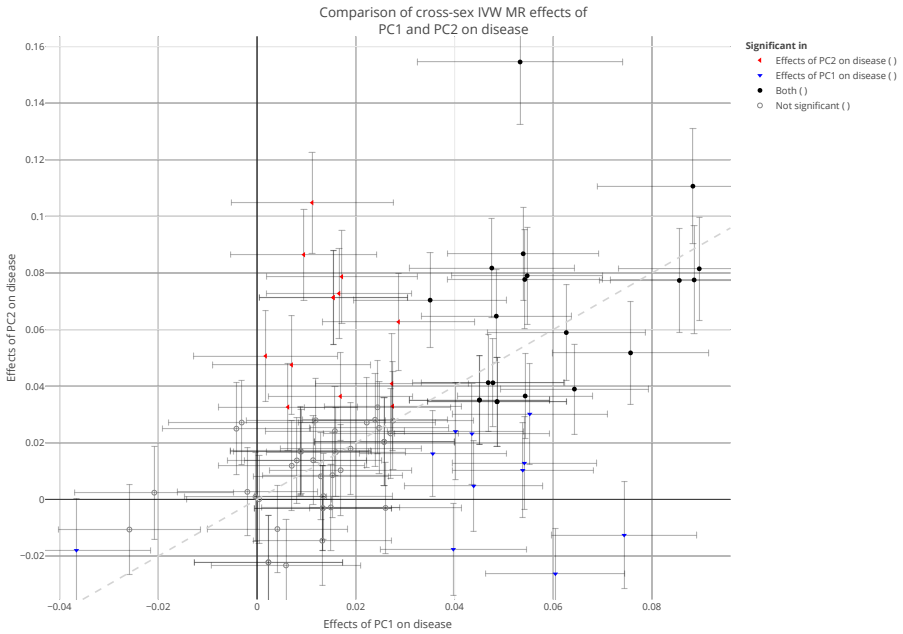

Supplementary figure 5: Comparison of effects of PC1 and PC2 on diseases estimated using cross-sex inverse-variance weighted (IVW) Mendelian randomization (MR) (X-axis) and weighted median MR (Y-axis). Each point is a distinct outcome, its coordinates showing the estimated causal effects from both methods. All summary statistics were calculated in the UK Biobank. The error bars show the 95 confidence interval.

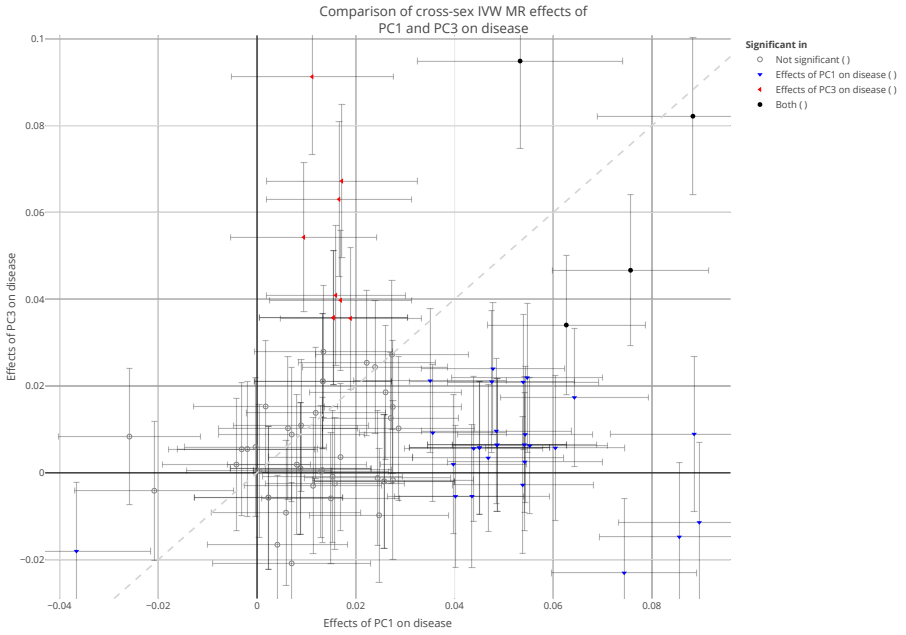

Supplementary figure 6: Comparison of effects of PC1 and PC3 on diseases estimated using cross-sex inverse-variance weighted (IVW) Mendelian randomization (MR) (X-axis) and weighted median MR (Y-axis). Each point is a distinct outcome, its coordinates showing the estimated causal effects from both methods. All summary statistics were calculated in the UK Biobank. The error bars show the 95 confidence interval.

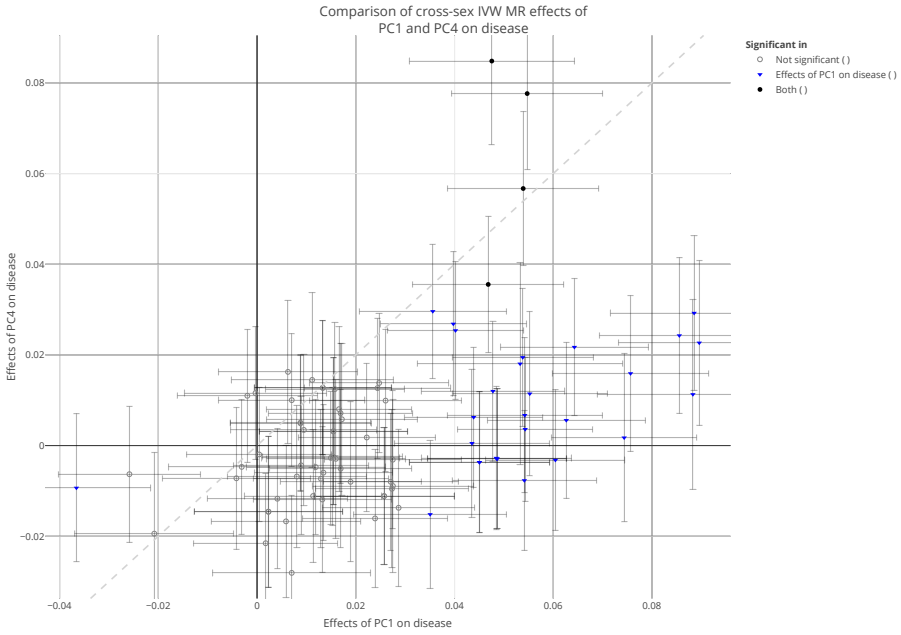

Supplementary figure 7: Comparison of effects of PC1 and PC4 on diseases estimated using cross-sex inverse-variance weighted (IVW) Mendelian randomization (MR) (X-axis) and weighted median MR (Y-axis). Each point is a distinct outcome, its coordinates showing the estimated causal effects from both methods. All summary statistics were calculated in the UK Biobank. The error bars show the 95 confidence interval.

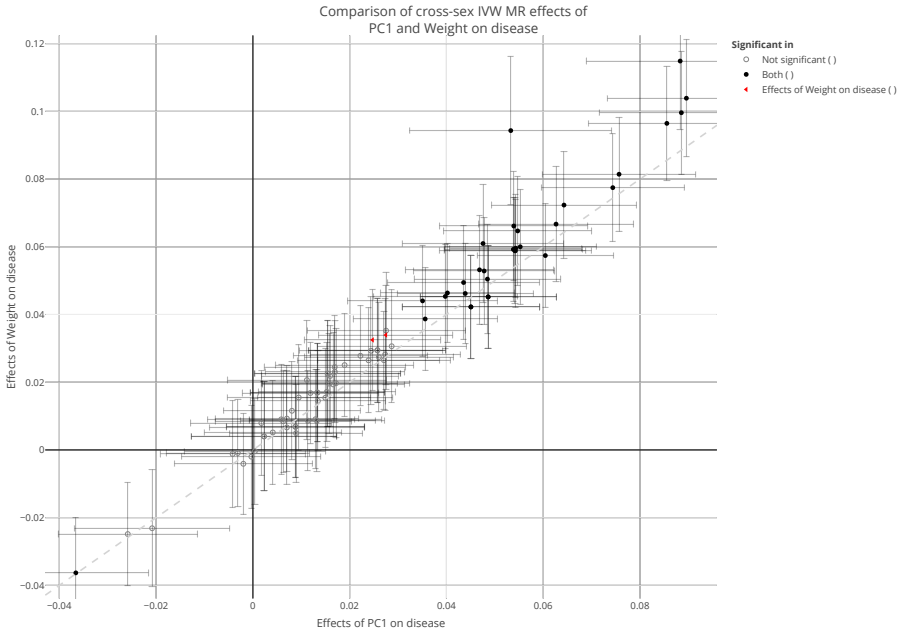

Supplementary figure 8: Comparison of effects of PC1 and weight on diseases estimated using cross-sex inverse-variance weighted (IVW) Mendelian randomization (MR) (X-axis) and weighted median MR (Y-axis). Each point is a distinct outcome, its coordinates showing the estimated causal effects from both methods. All summary statistics were calculated in the UK Biobank. The error bars show the 95 confidence interval.

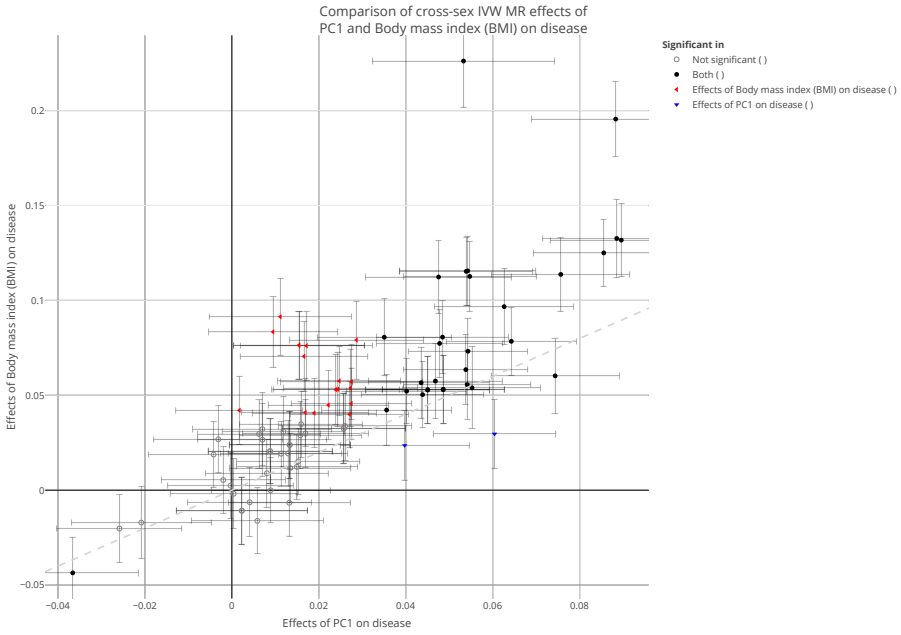

Supplementary figure 9: Comparison of effects of PC1 and BMI on diseases estimated using cross-sex inverse-variance weighted (IVW) Mendelian randomization (MR) (X-axis) and weighted median MR (Y-axis). Each point is a distinct outcome, its coordinates showing the estimated causal effects from both methods. All summary statistics were calculated in the UK Biobank. The error bars show the 95 confidence interval.

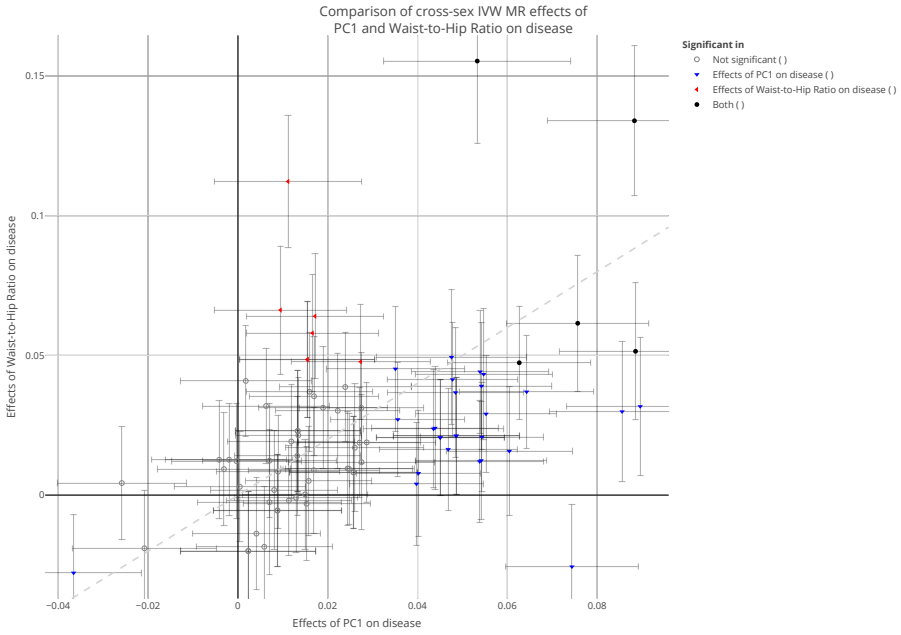

Supplementary figure 10: Comparison of effects of PC1 and WHR on diseases estimated using cross-sex inverse-variance weighted (IVW) Mendelian randomization (MR) (X-axis) and weighted median MR (Y-axis). Each point is a distinct outcome, its coordinates showing the estimated causal effects from both methods. All summary statistics were calculated in the UK Biobank. The error bars show the 95 confidence interval.

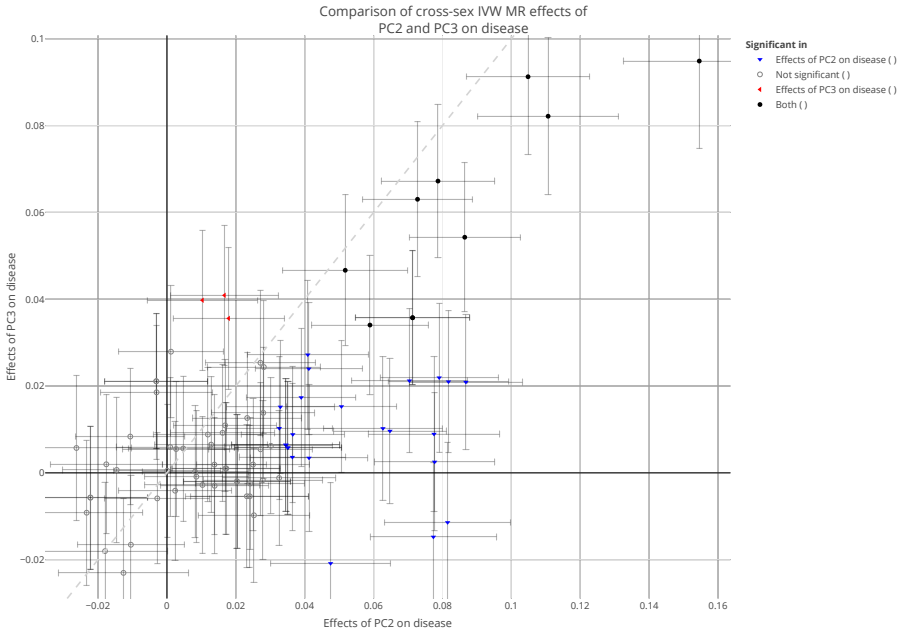

Supplementary figure 11: Comparison of effects of PC2 and PC3 on diseases estimated using cross-sex inverse-variance weighted (IVW) Mendelian randomization (MR) (X-axis) and weighted median MR (Y-axis). Each point is a distinct outcome, its coordinates showing the estimated causal effects from both methods. All summary statistics were calculated in the UK Biobank. The error bars show the 95 confidence interval.

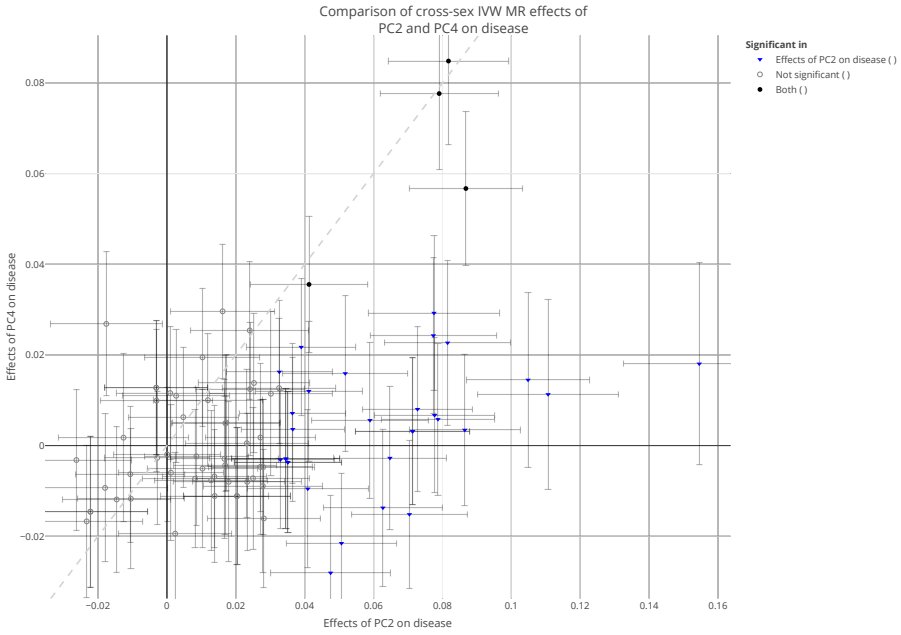

Supplementary figure 12: Comparison of effects of PC2 and PC4 on diseases estimated using cross-sex inverse-variance weighted (IVW) Mendelian randomization (MR) (X-axis) and weighted median MR (Y-axis). Each point is a distinct outcome, its coordinates showing the estimated causal effects from both methods. All summary statistics were calculated in the UK Biobank. The error bars show the 95 confidence interval.

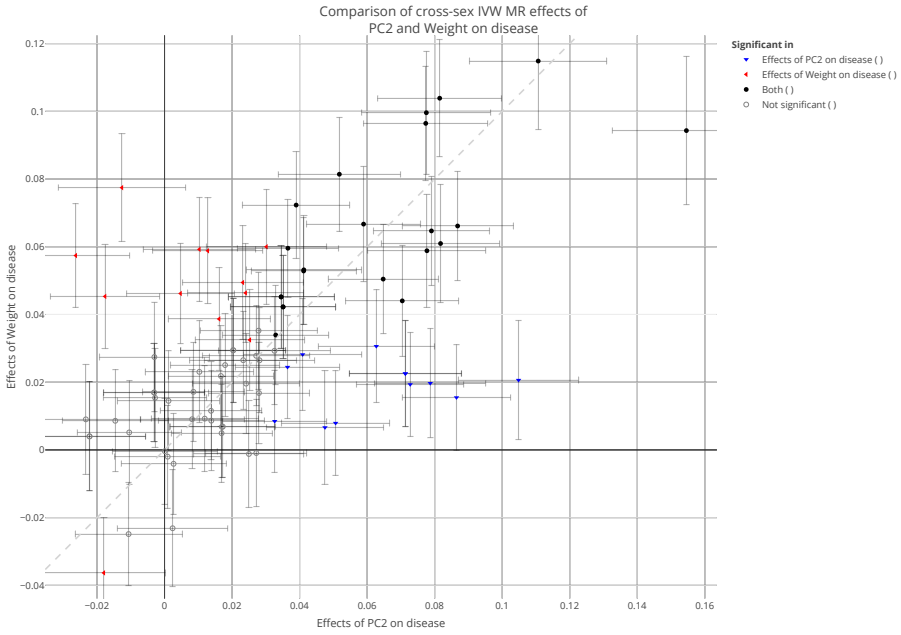

Supplementary figure 13: Comparison of effects of PC2 and weight on diseases estimated using cross-sex inverse-variance weighted (IVW) Mendelian randomization (MR) (X-axis) and weighted median MR (Y-axis). Each point is a distinct outcome, its coordinates showing the estimated causal effects from both methods. All summary statistics were calculated in the UK Biobank. The error bars show the 95 confidence interval.

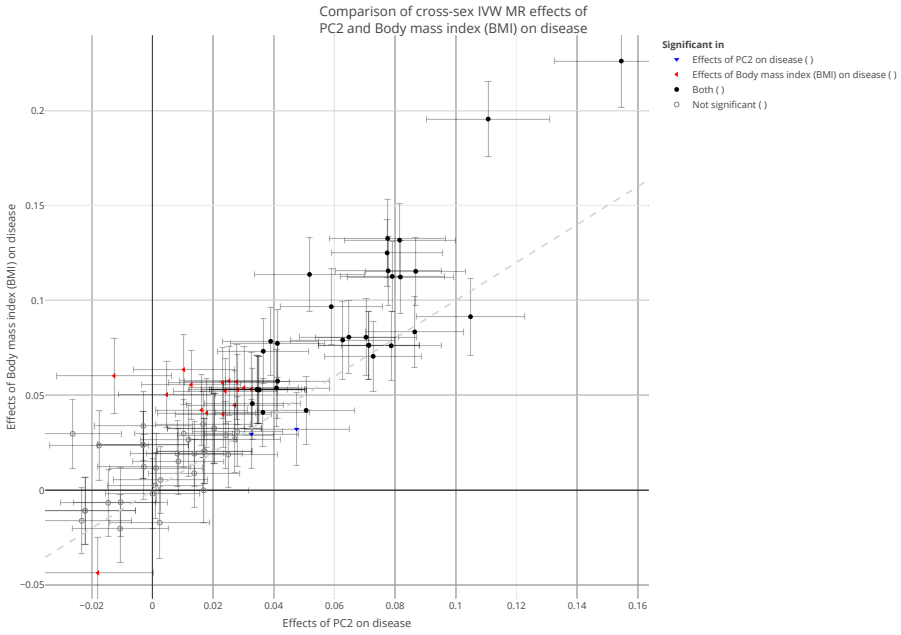

Supplementary figure 14: Comparison of effects of PC2 and BMI on diseases estimated using cross-sex inverse-variance weighted (IVW) Mendelian randomization (MR) (X-axis) and weighted median MR (Y-axis). Each point is a distinct outcome, its coordinates showing the estimated causal effects from both methods. All summary statistics were calculated in the UK Biobank. The error bars show the 95 confidence interval.

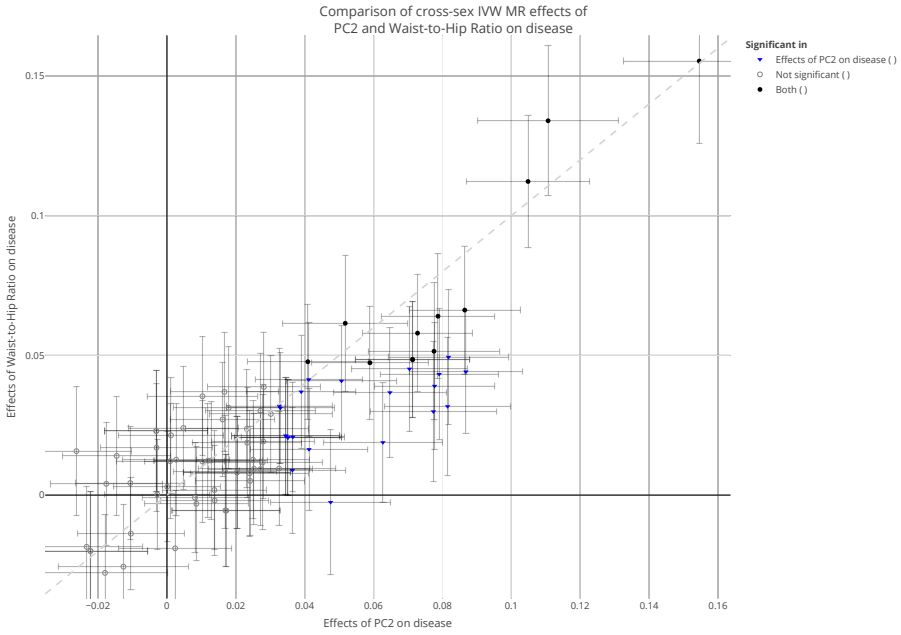

Supplementary figure 15: Comparison of effects of PC2 and WHR on diseases estimated using cross-sex inverse-variance weighted (IVW) Mendelian randomization (MR) (X-axis) and weighted median MR (Y-axis). Each point is a distinct outcome, its coordinates showing the estimated causal effects from both methods. All summary statistics were calculated in the UK Biobank. The error bars show the 95 confidence interval.

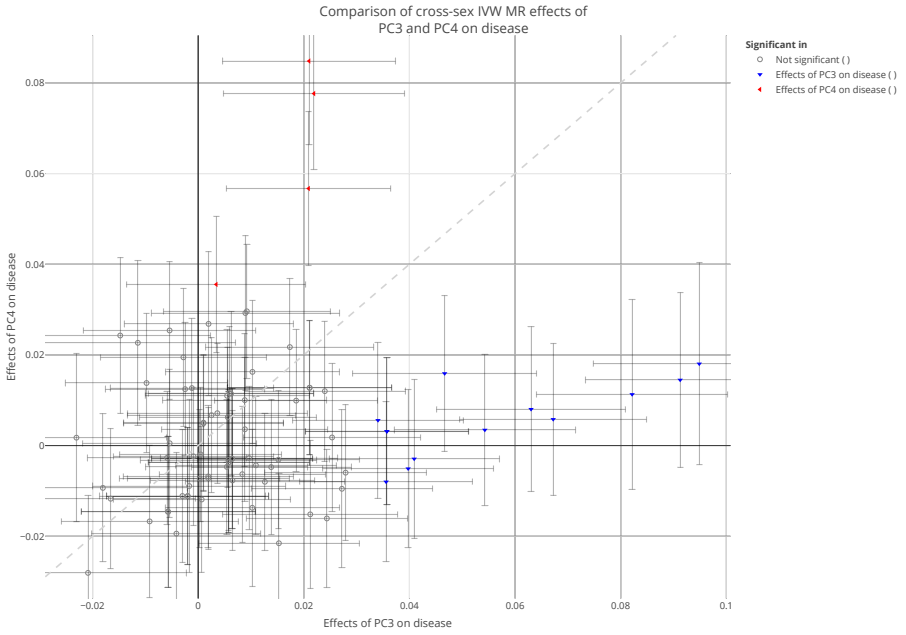

Supplementary figure 16: Comparison of effects of PC3 and PC4 on diseases estimated using cross-sex inverse-variance weighted (IVW) Mendelian randomization (MR) (X-axis) and weighted median MR (Y-axis). Each point is a distinct outcome, its coordinates showing the estimated causal effects from both methods. All summary statistics were calculated in the UK Biobank. The error bars show the 95 confidence interval.

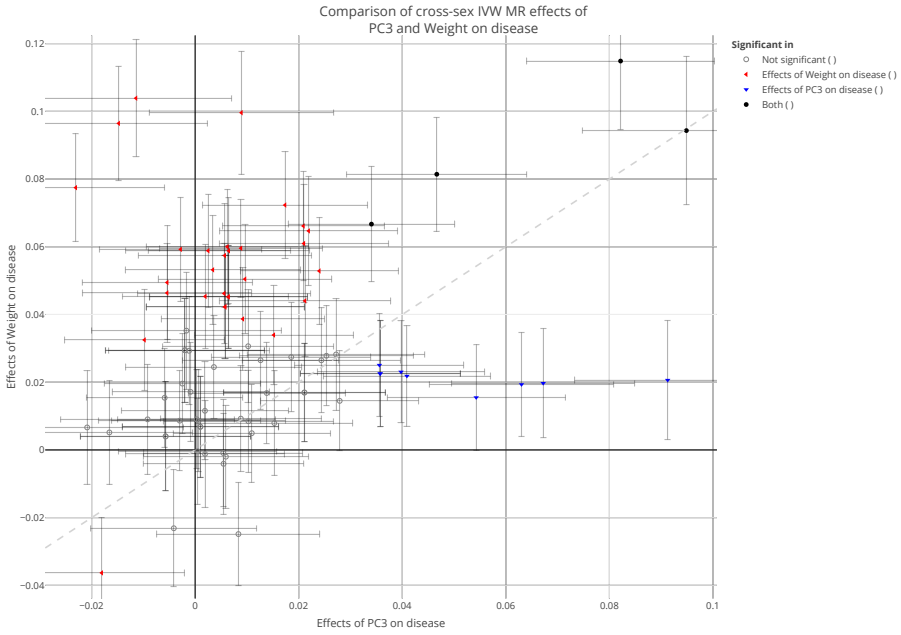

Supplementary figure 17: Comparison of effects of PC3 and weight on diseases estimated using cross-sex inverse-variance weighted (IVW) Mendelian randomization (MR) (X-axis) and weighted median MR (Y-axis). Each point is a distinct outcome, its coordinates showing the estimated causal effects from both methods. All summary statistics were calculated in the UK Biobank. The error bars show the 95 confidence interval.

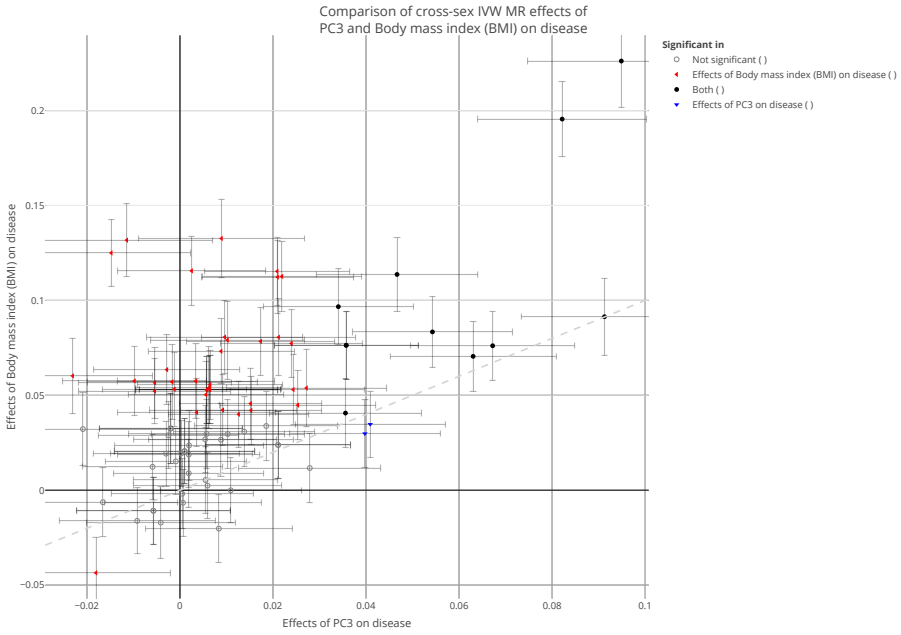

Supplementary figure 18: Comparison of effects of PC3 and BMI on diseases estimated using cross-sex inverse-variance weighted (IVW) Mendelian randomization (MR) (X-axis) and weighted median MR (Y-axis). Each point is a distinct outcome, its coordinates showing the estimated causal effects from both methods. All summary statistics were calculated in the UK Biobank. The error bars show the 95 confidence interval.

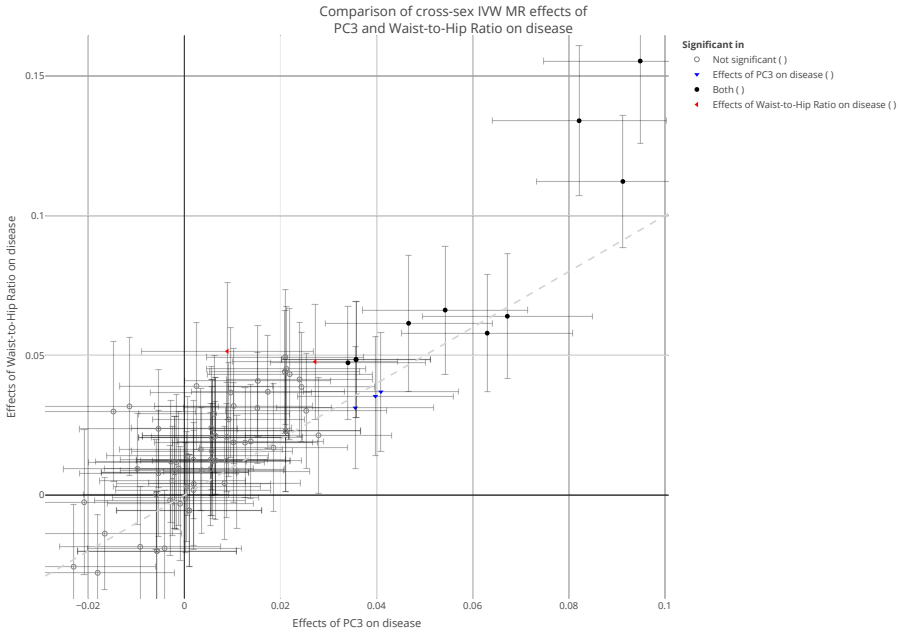

Supplementary figure 19: Comparison of effects of PC3 and WHR on diseases estimated using cross-sex inverse-variance weighted (IVW) Mendelian randomization (MR) (X-axis) and weighted median MR (Y-axis). Each point is a distinct outcome, its coordinates showing the estimated causal effects from both methods. All summary statistics were calculated in the UK Biobank. The error bars show the 95 confidence interval.

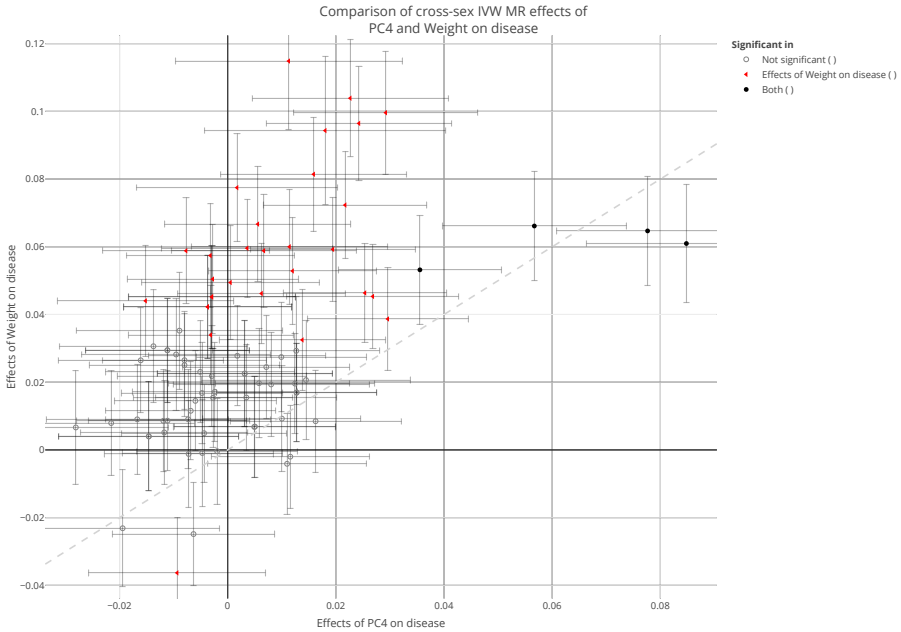

Supplementary figure 20: Comparison of effects of PC4 and weight on diseases estimated using cross-sex inverse-variance weighted (IVW) Mendelian randomization (MR) (X-axis) and weighted median MR (Y-axis). Each point is a distinct outcome, its coordinates showing the estimated causal effects from both methods. All summary statistics were calculated in the UK Biobank. The error bars show the 95 confidence interval.

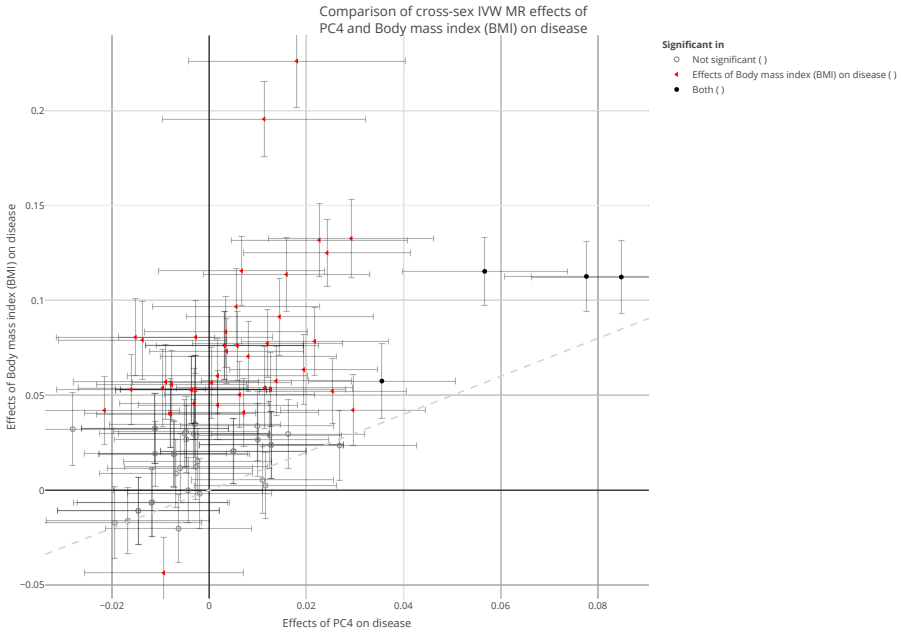

Supplementary figure 21: Comparison of effects of PC4 and BMI on diseases estimated using cross-sex inverse-variance weighted (IVW) Mendelian randomization (MR) (X-axis) and weighted median MR (Y-axis). Each point is a distinct outcome, its coordinates showing the estimated causal effects from both methods. All summary statistics were calculated in the UK Biobank. The error bars show the 95 confidence interval.

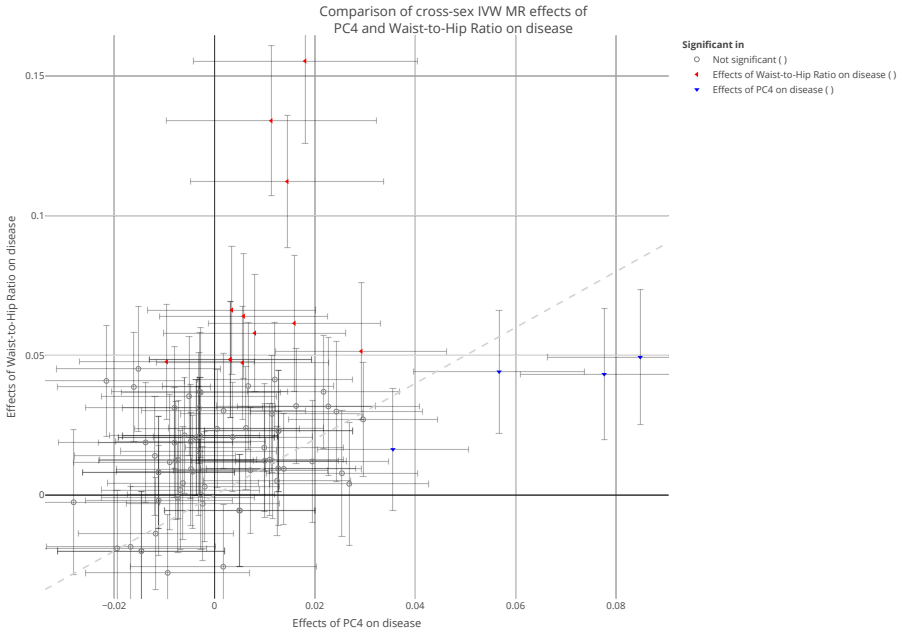

Supplementary figure 22: Comparison of effects of PC4 and WHR on diseases estimated using cross-sex inverse-variance weighted (IVW) Mendelian randomization (MR) (X-axis) and weighted median MR (Y-axis). Each point is a distinct outcome, its coordinates showing the estimated causal effects from both methods. All summary statistics were calculated in the UK Biobank. The error bars show the 95 confidence interval.

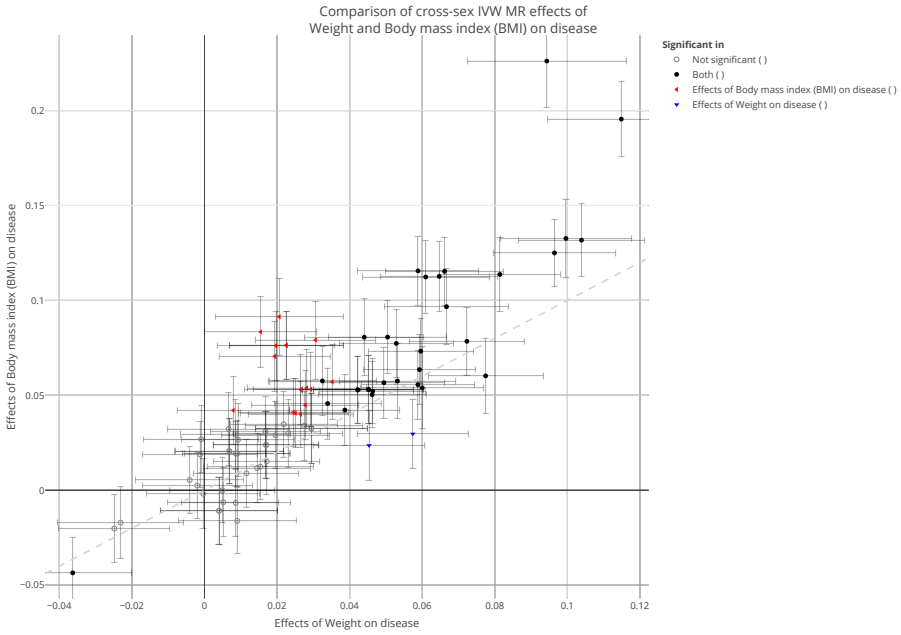

Supplementary figure 23: Comparison of effects of weight and BMI on diseases estimated using cross-sex inverse-variance weighted (IVW) Mendelian randomization (MR) (X-axis) and weighted median MR (Y-axis). Each point is a distinct outcome, its coordinates showing the estimated causal effects from both methods. All summary statistics were calculated in the UK Biobank. The error bars show the 95 confidence interval.

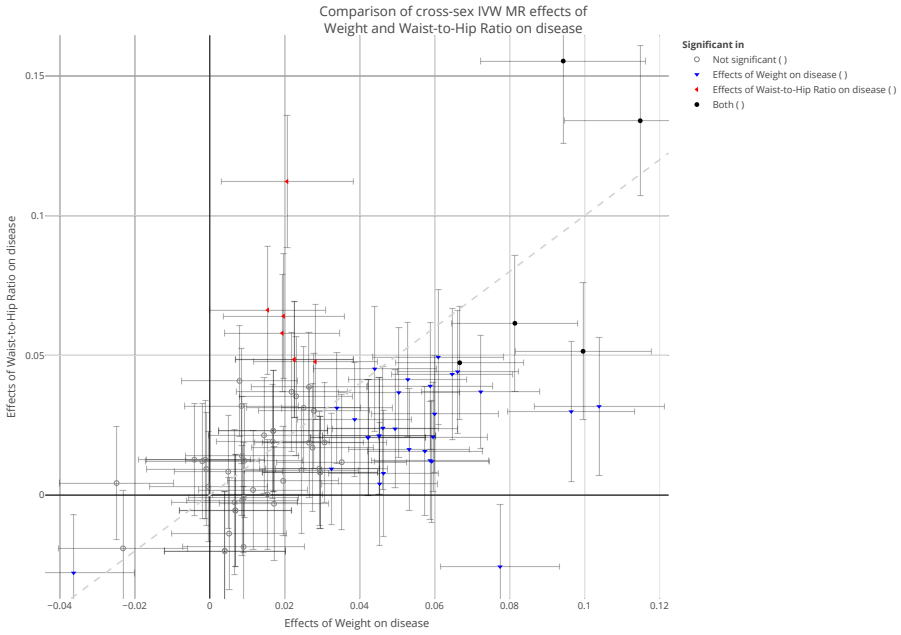

Supplementary figure 24: Comparison of effects of weight and WHR on diseases estimated using cross-sex inverse-variance weighted (IVW) Mendelian randomization (MR) (X-axis) and weighted median MR (Y-axis). Each point is a distinct outcome, its coordinates showing the estimated causal effects from both methods. All summary statistics were calculated in the UK Biobank. The error bars show the 95 confidence interval.

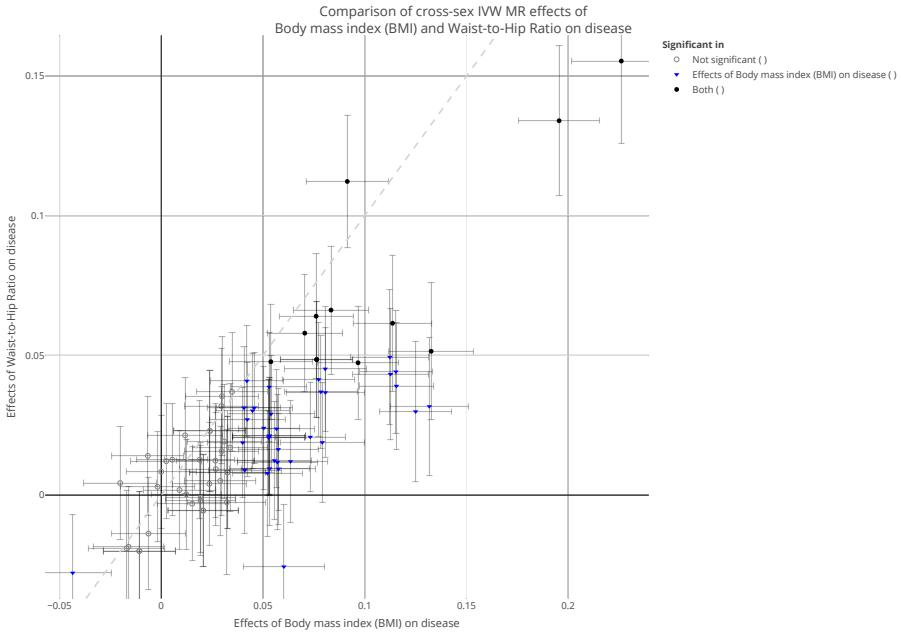

Supplementary figure 25: Comparison of effects of BMI and WHR on diseases estimated using cross-sex inverse-variance weighted (IVW) Mendelian randomization (MR) (X-axis) and weighted median MR (Y-axis). Each point is a distinct outcome, its coordinates showing the estimated causal effects from both methods. All summary statistics were calculated in the UK Biobank. The error bars show the 95 confidence interval.

4.2 Effects on lifestyle phenotypes

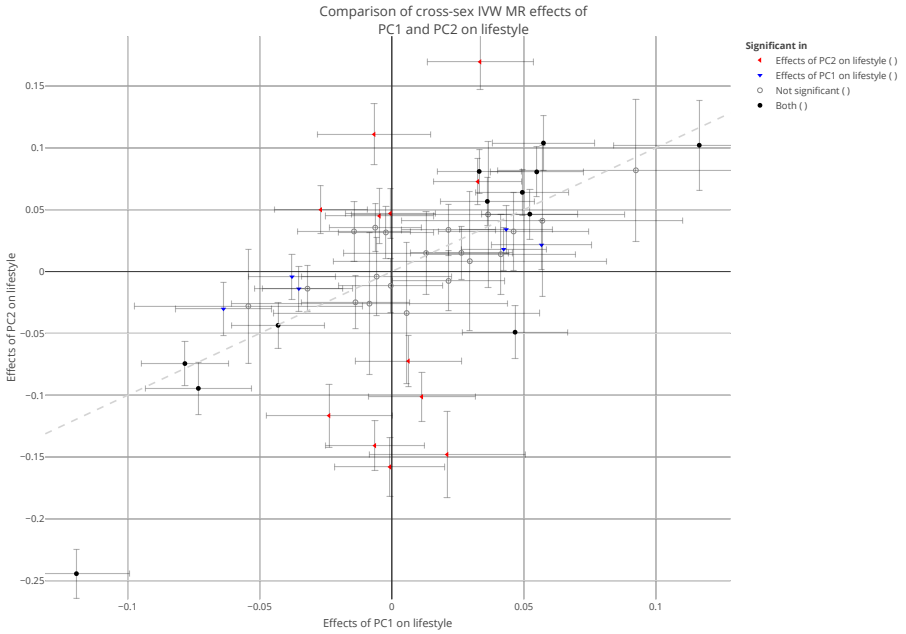

Supplementary figure 26: Comparison of effects of PC1 and PC2 on lifestyle phenotypes estimated using cross-sex inverse-variance weighted (IVW) Mendelian randomization (MR) (X-axis) and weighted median MR (Y-axis). Each point is a distinct outcome, its coordinates showing the estimated causal effects from both methods. All summary statistics were calculated in the UK Biobank. The error bars show the 95 confidence interval.

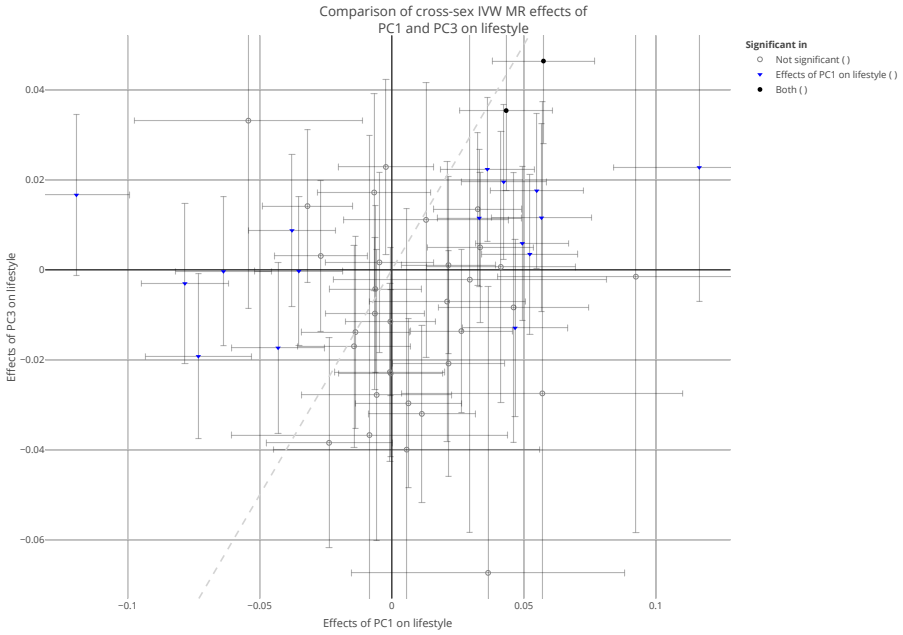

Supplementary figure 27: Comparison of effects of PC1 and PC3 on lifestyle phenotypes estimated using cross-sex inverse-variance weighted (IVW) Mendelian randomization (MR) (X-axis) and weighted median MR (Y-axis). Each point is a distinct outcome, its coordinates showing the estimated causal effects from both methods. All summary statistics were calculated in the UK Biobank. The error bars show the 95 confidence interval.

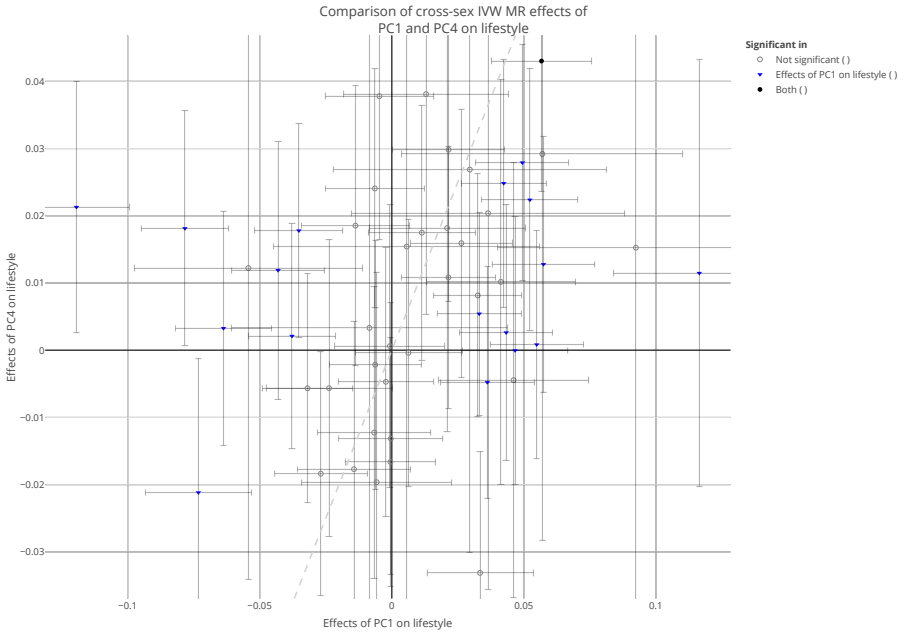

Supplementary figure 28: Comparison of effects of PC1 and PC4 on lifestyle phenotypes estimated using cross-sex inverse-variance weighted (IVW) Mendelian randomization (MR) (X-axis) and weighted median MR (Y-axis). Each point is a distinct outcome, its coordinates showing the estimated causal effects from both methods. All summary statistics were calculated in the UK Biobank. The error bars show the 95 confidence interval.

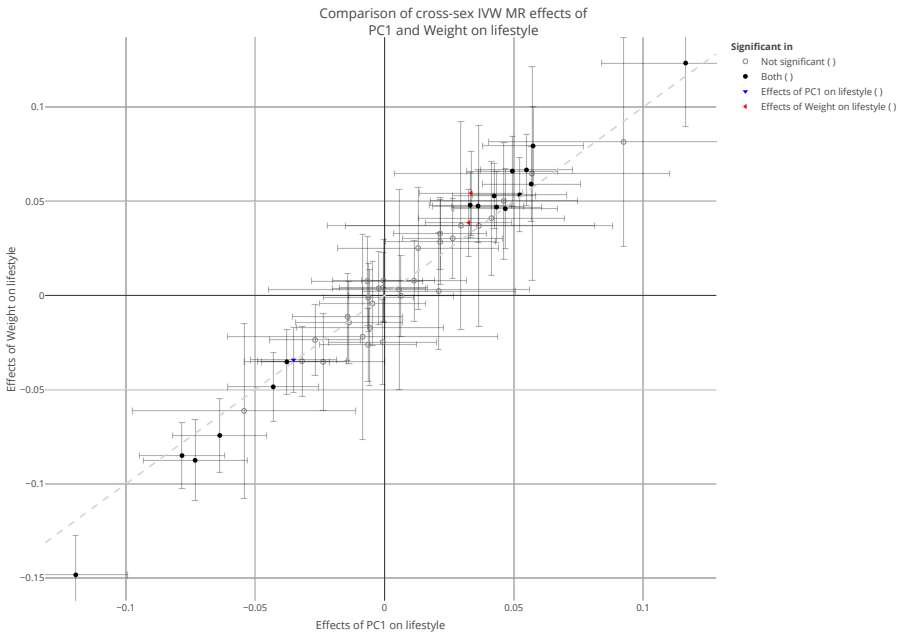

Supplementary figure 29: Comparison of effects of PC1 and weight on lifestyle phenotypes estimated using cross-sex inverse-variance weighted (IVW) Mendelian randomization (MR) (X-axis) and weighted median MR (Y-axis). Each point is a distinct outcome, its coordinates showing the estimated causal effects from both methods. All summary statistics were calculated in the UK Biobank. The error bars show the 95 confidence interval.

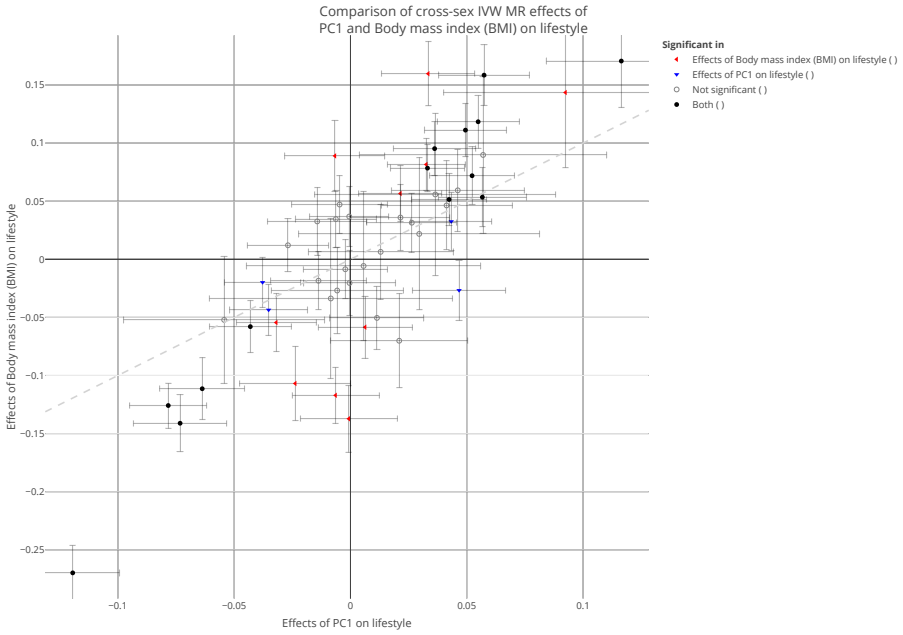

Supplementary figure 30: Comparison of effects of PC1 and BMI on lifestyle phenotypes estimated using cross-sex inverse-variance weighted (IVW) Mendelian randomization (MR) (X-axis) and weighted median MR (Y-axis). Each point is a distinct outcome, its coordinates showing the estimated causal effects from both methods. All summary statistics were calculated in the UK Biobank. The error bars show the 95 confidence interval.

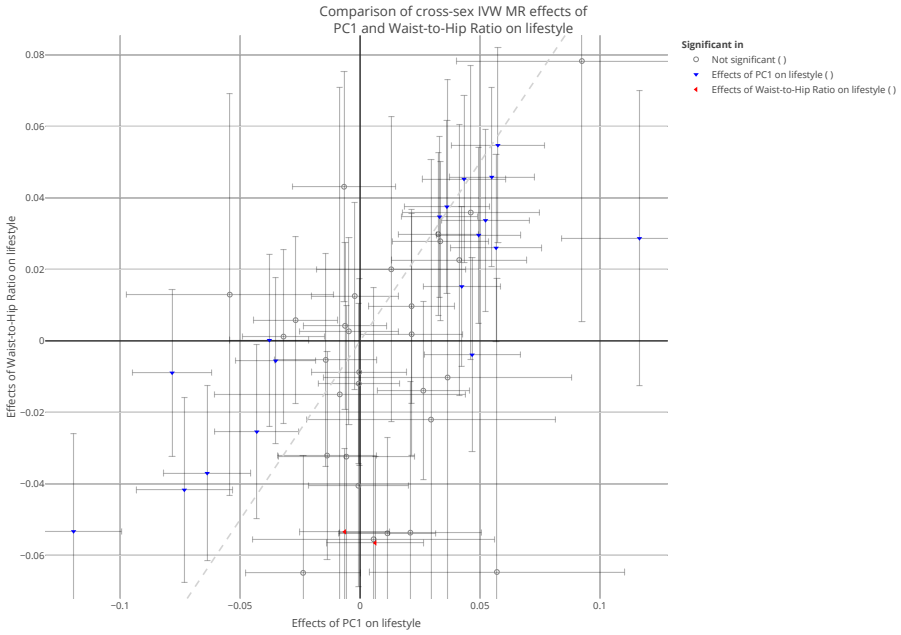

Supplementary figure 31: Comparison of effects of PC1 and WHR on lifestyle phenotypes estimated using cross-sex inverse-variance weighted (IVW) Mendelian randomization (MR) (X-axis) and weighted median MR (Y-axis). Each point is a distinct outcome, its coordinates showing the estimated causal effects from both methods. All summary statistics were calculated in the UK Biobank. The error bars show the 95 confidence interval.

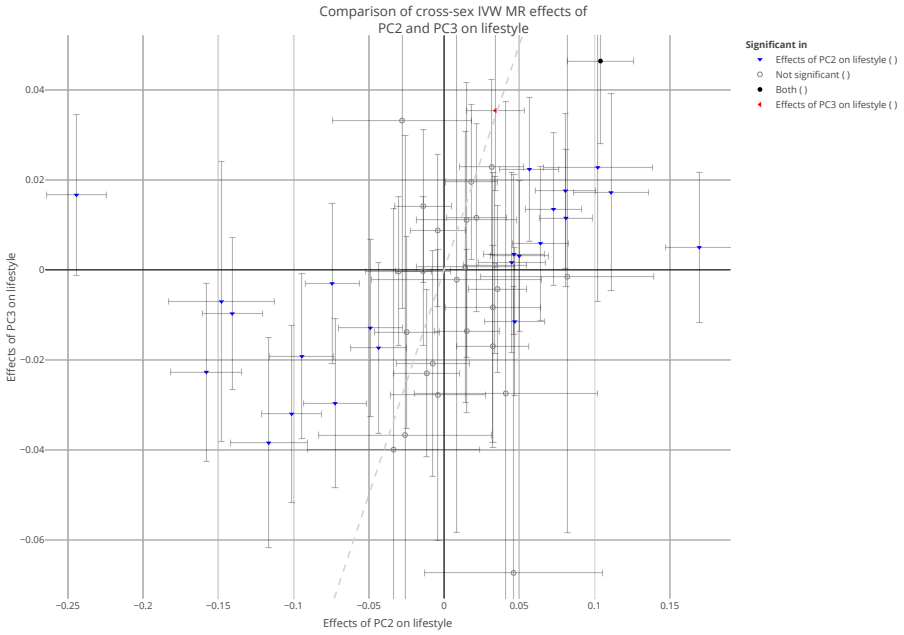

Supplementary figure 32: Comparison of effects of PC2 and PC3 on lifestyle phenotypes estimated using cross-sex inverse-variance weighted (IVW) Mendelian randomization (MR) (X-axis) and weighted median MR (Y-axis). Each point is a distinct outcome, its coordinates showing the estimated causal effects from both methods. All summary statistics were calculated in the UK Biobank. The error bars show the 95 confidence interval.

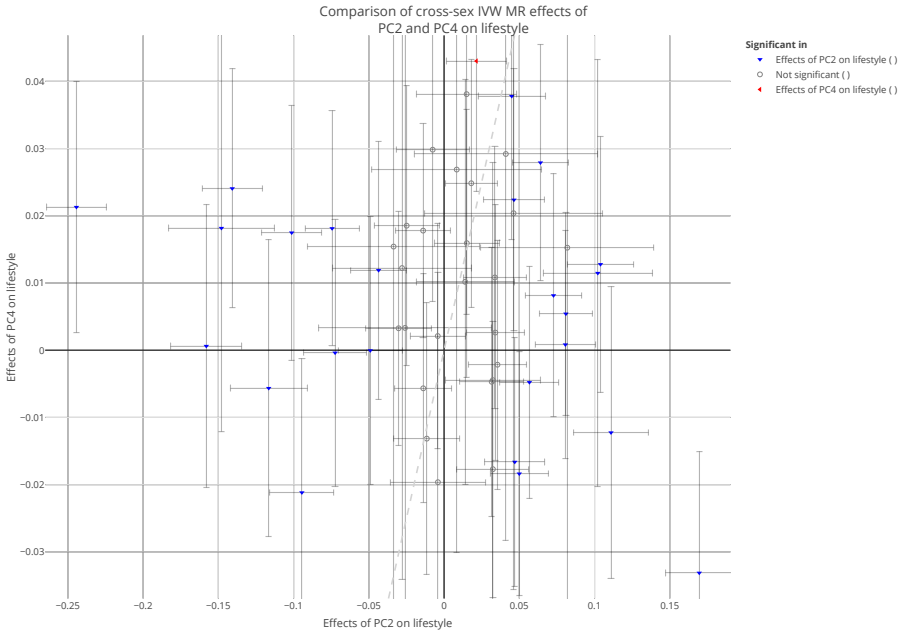

Supplementary figure 33: Comparison of effects of PC2 and PC4 on lifestyle phenotypes estimated using cross-sex inverse-variance weighted (IVW) Mendelian randomization (MR) (X-axis) and weighted median MR (Y-axis). Each point is a distinct outcome, its coordinates showing the estimated causal effects from both methods. All summary statistics were calculated in the UK Biobank. The error bars show the 95 confidence interval.

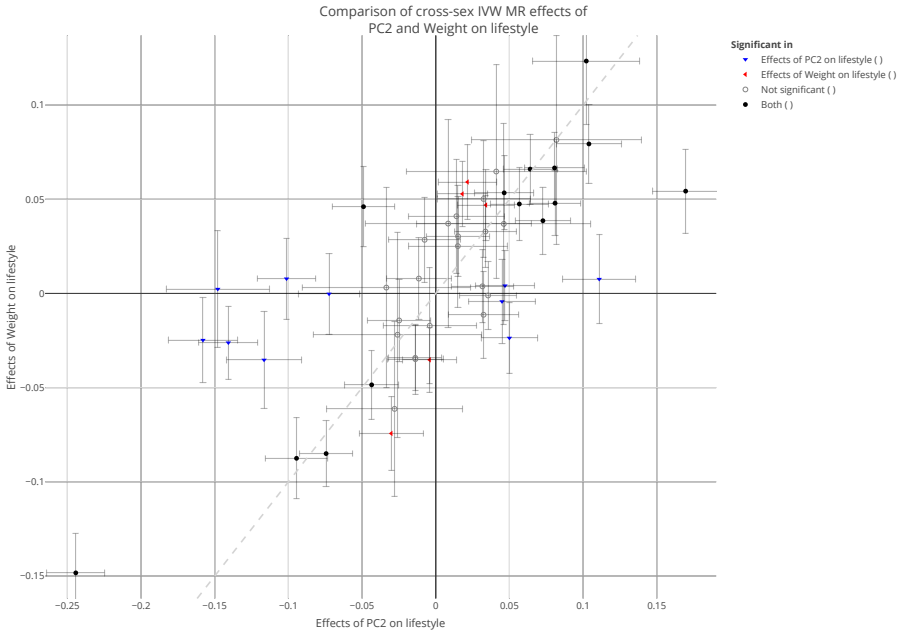

Supplementary figure 34: Comparison of effects of PC2 and weight on lifestyle phenotypes estimated using cross-sex inverse-variance weighted (IVW) Mendelian randomization (MR) (X-axis) and weighted median MR (Y-axis). Each point is a distinct outcome, its coordinates showing the estimated causal effects from both methods. All summary statistics were calculated in the UK Biobank. The error bars show the 95 confidence interval.

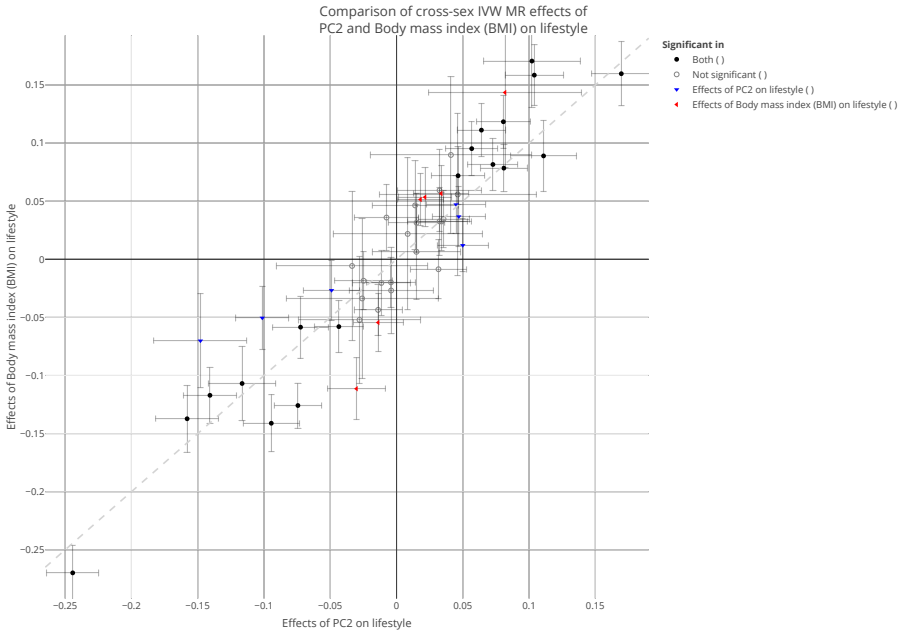

Supplementary figure 35: Comparison of effects of PC2 and BMI on lifestyle phenotypes estimated using cross-sex inverse-variance weighted (IVW) Mendelian randomization (MR) (X-axis) and weighted median MR (Y-axis). Each point is a distinct outcome, its coordinates showing the estimated causal effects from both methods. All summary statistics were calculated in the UK Biobank. The error bars show the 95 confidence interval.

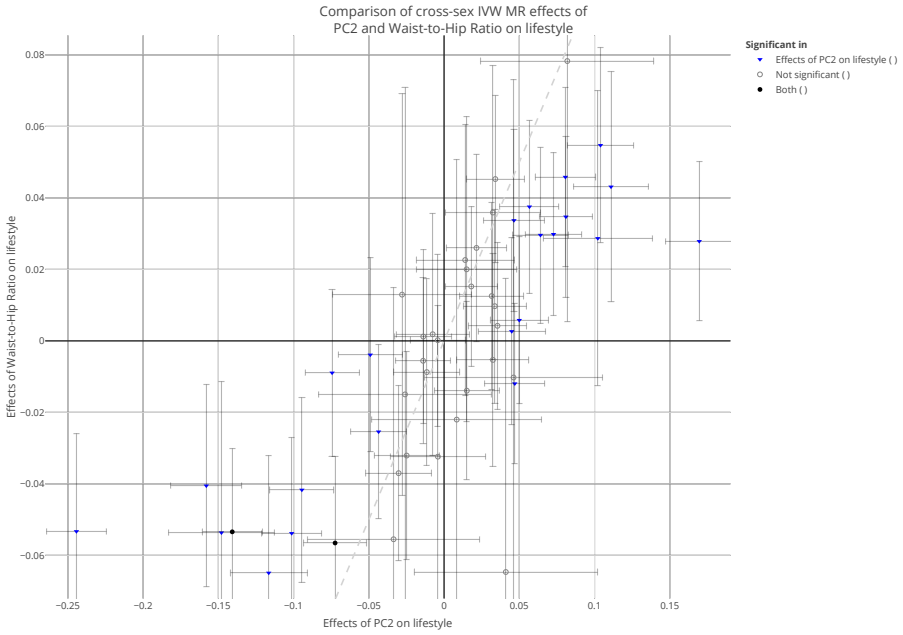

Supplementary figure 36: Comparison of effects of PC2 and WHR on lifestyle phenotypes estimated using cross-sex inverse-variance weighted (IVW) Mendelian randomization (MR) (X-axis) and weighted median MR (Y-axis). Each point is a distinct outcome, its coordinates showing the estimated causal effects from both methods. All summary statistics were calculated in the UK Biobank. The error bars show the 95 confidence interval.

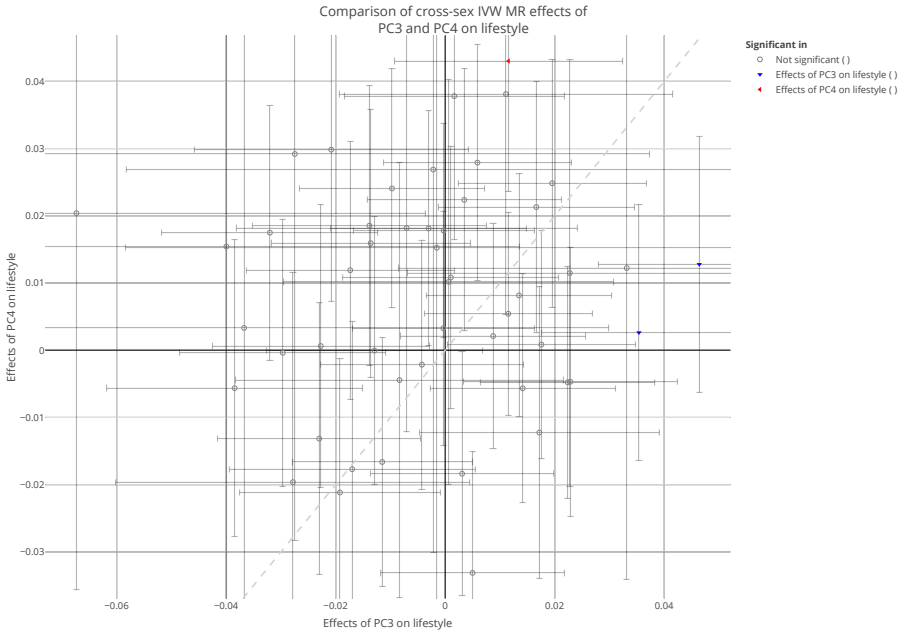

Supplementary figure 37: Comparison of effects of PC3 and PC4 on lifestyle phenotypes estimated using cross-sex inverse-variance weighted (IVW) Mendelian randomization (MR) (X-axis) and weighted median MR (Y-axis). Each point is a distinct outcome, its coordinates showing the estimated causal effects from both methods. All summary statistics were calculated in the UK Biobank. The error bars show the 95 confidence interval.

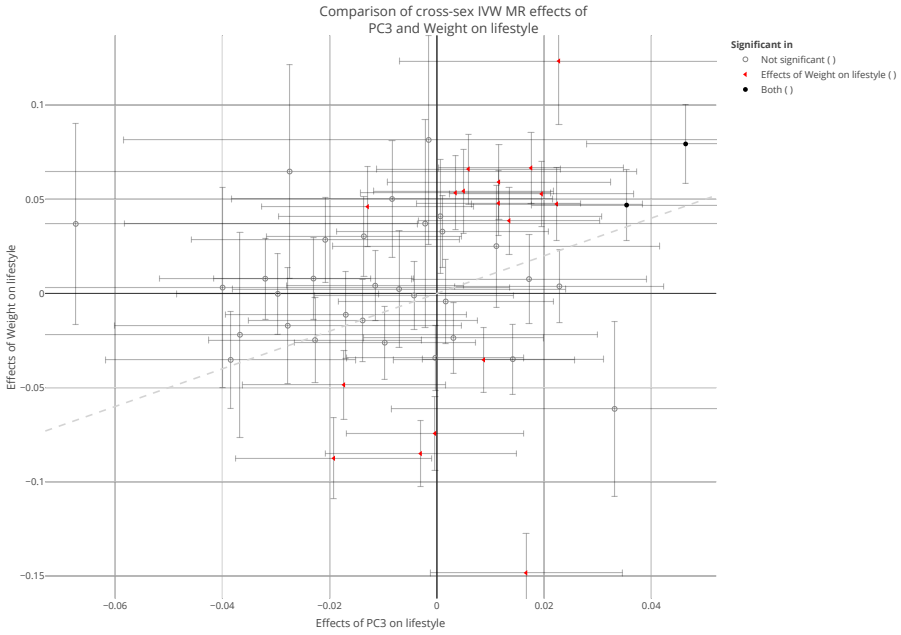

Supplementary figure 38: Comparison of effects of PC3 and weight on lifestyle phenotypes estimated using cross-sex inverse-variance weighted (IVW) Mendelian randomization (MR) (X-axis) and weighted median MR (Y-axis). Each point is a distinct outcome, its coordinates showing the estimated causal effects from both methods. All summary statistics were calculated in the UK Biobank. The error bars show the 95 confidence interval.

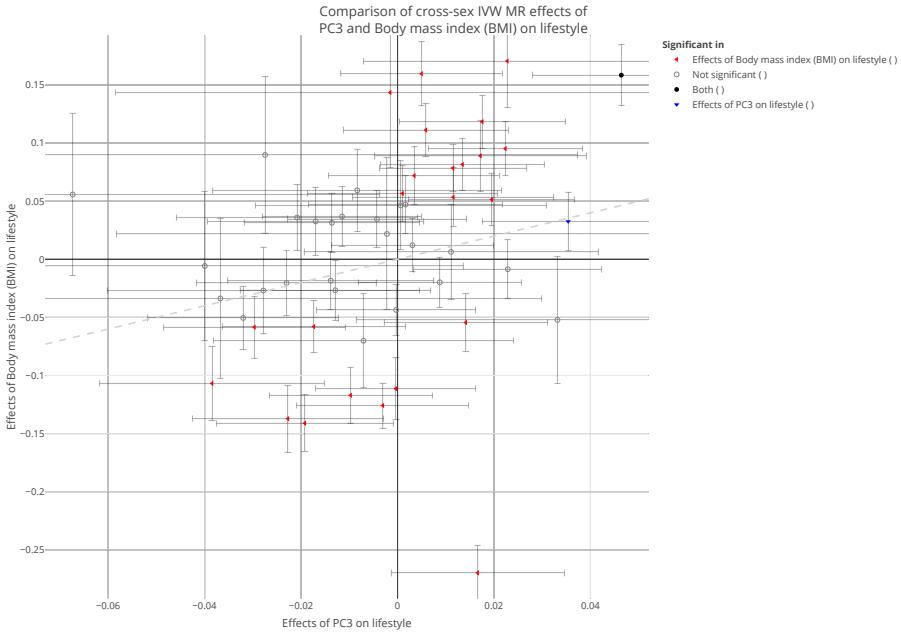

Supplementary figure 39: Comparison of effects of PC3 and BMI on lifestyle phenotypes estimated using cross-sex inverse-variance weighted (IVW) Mendelian randomization (MR) (X-axis) and weighted median MR (Y-axis). Each point is a distinct outcome, its coordinates showing the estimated causal effects from both methods. All summary statistics were calculated in the UK Biobank. The error bars show the 95 confidence interval.

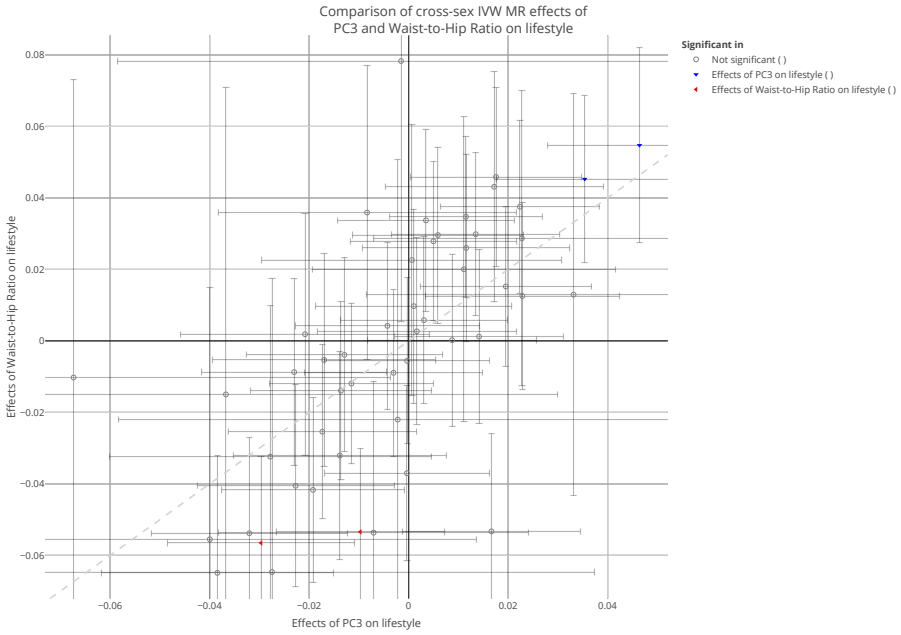

Supplementary figure 40: Comparison of effects of PC3 and WHR on lifestyle phenotypes estimated using cross-sex inverse-variance weighted (IVW) Mendelian randomization (MR) (X-axis) and weighted median MR (Y-axis). Each point is a distinct outcome, its coordinates showing the estimated causal effects from both methods. All summary statistics were calculated in the UK Biobank. The error bars show the 95 confidence interval.

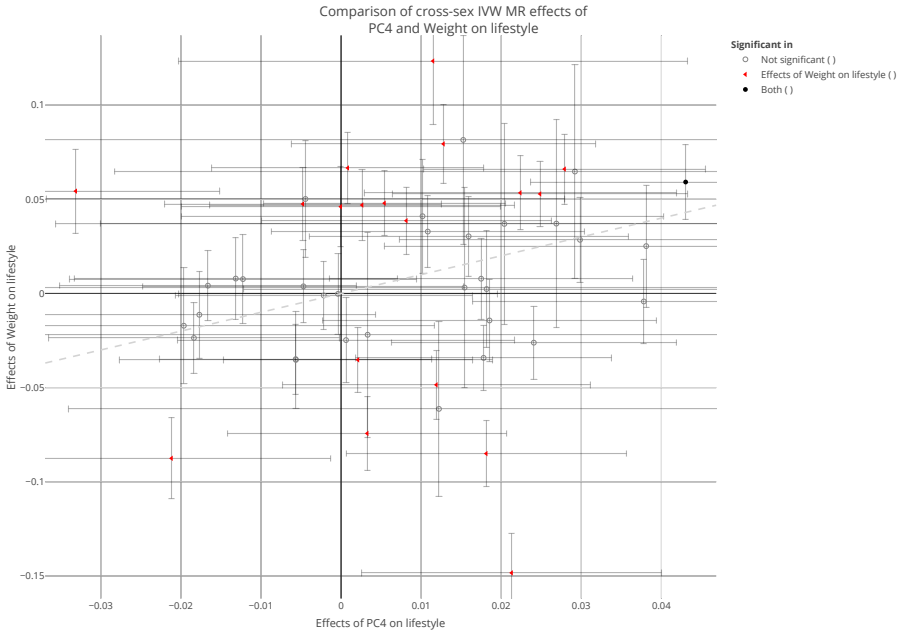

Supplementary figure 41: Comparison of effects of PC4 and weight on lifestyle phenotypes estimated using cross-sex inverse-variance weighted (IVW) Mendelian randomization (MR) (X-axis) and weighted median MR (Y-axis). Each point is a distinct outcome, its coordinates showing the estimated causal effects from both methods. All summary statistics were calculated in the UK Biobank. The error bars show the 95 confidence interval.

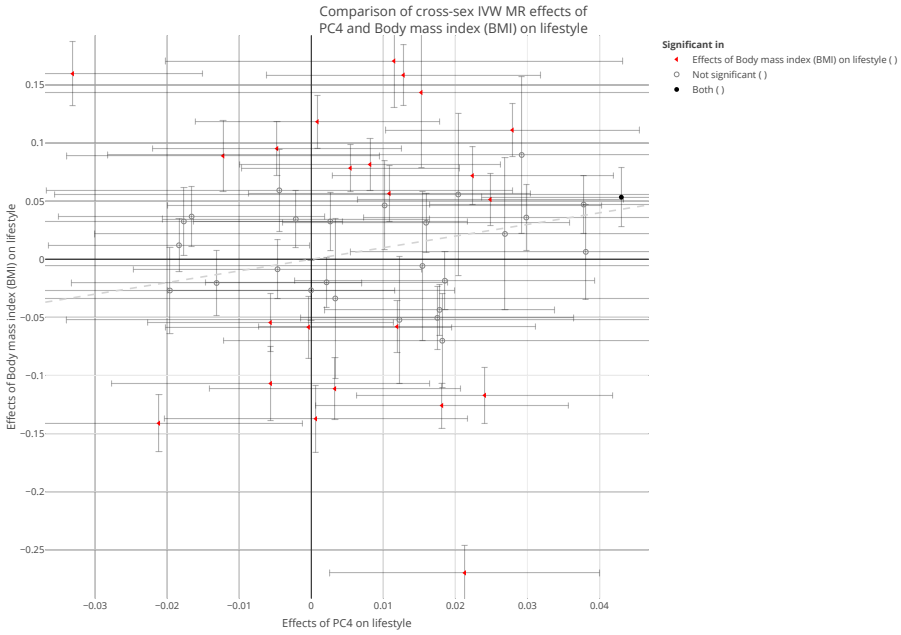

Supplementary figure 42: Comparison of effects of PC4 and BMI on lifestyle phenotypes estimated using cross-sex inverse-variance weighted (IVW) Mendelian randomization (MR) (X-axis) and weighted median MR (Y-axis). Each point is a distinct outcome, its coordinates showing the estimated causal effects from both methods. All summary statistics were calculated in the UK Biobank. The error bars show the 95 confidence interval.

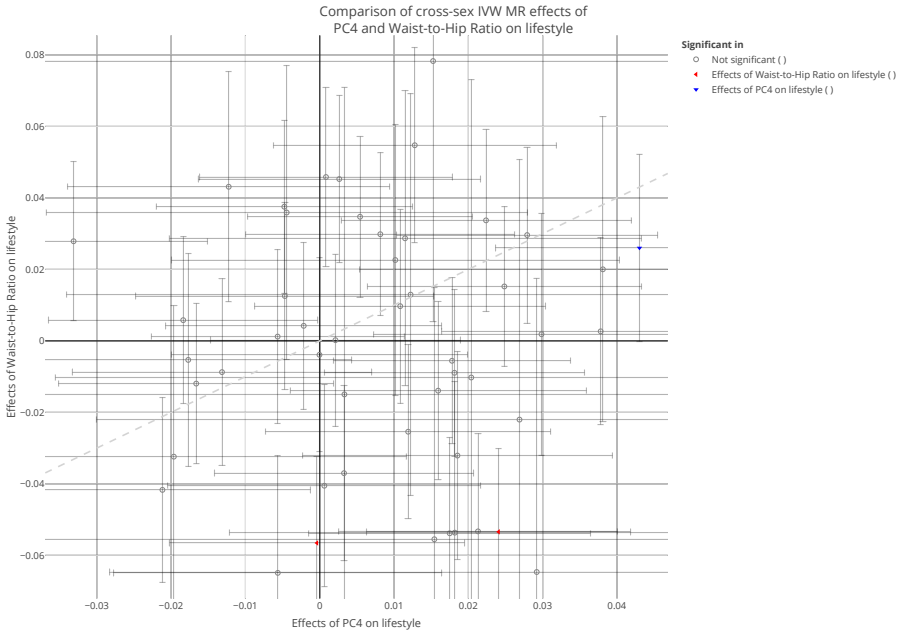

Supplementary figure 43: Comparison of effects of PC4 and WHR on lifestyle phenotypes estimated using cross-sex inverse-variance weighted (IVW) Mendelian randomization (MR) (X-axis) and weighted median MR (Y-axis). Each point is a distinct outcome, its coordinates showing the estimated causal effects from both methods. All summary statistics were calculated in the UK Biobank. The error bars show the 95 confidence interval.

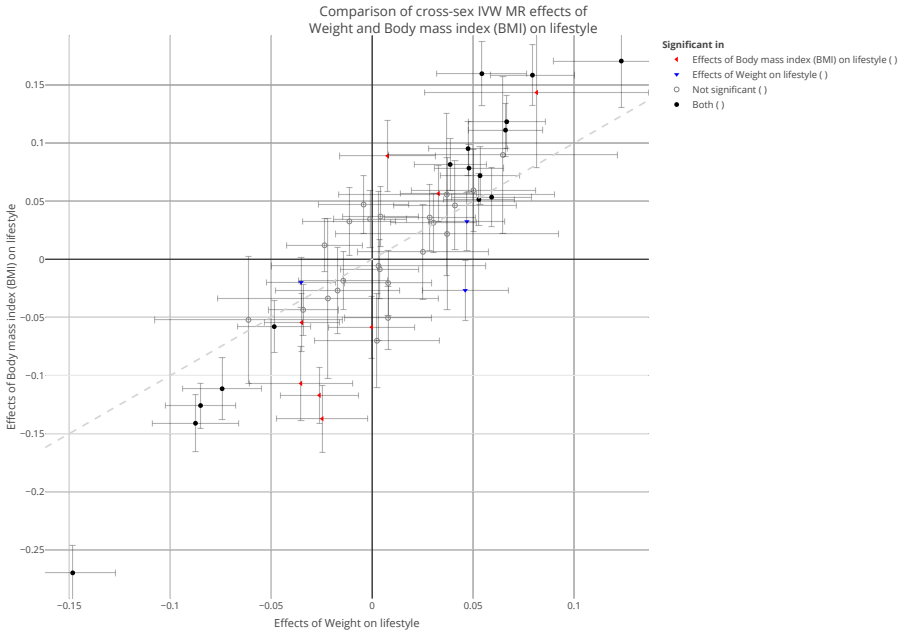

Supplementary figure 44: Comparison of effects of weight and BMI on lifestyle phenotypes estimated using cross-sex inverse-variance weighted (IVW) Mendelian randomization (MR) (X-axis) and weighted median MR (Y-axis). Each point is a distinct outcome, its coordinates showing the estimated causal effects from both methods. All summary statistics were calculated in the UK Biobank. The error bars show the 95 confidence interval.

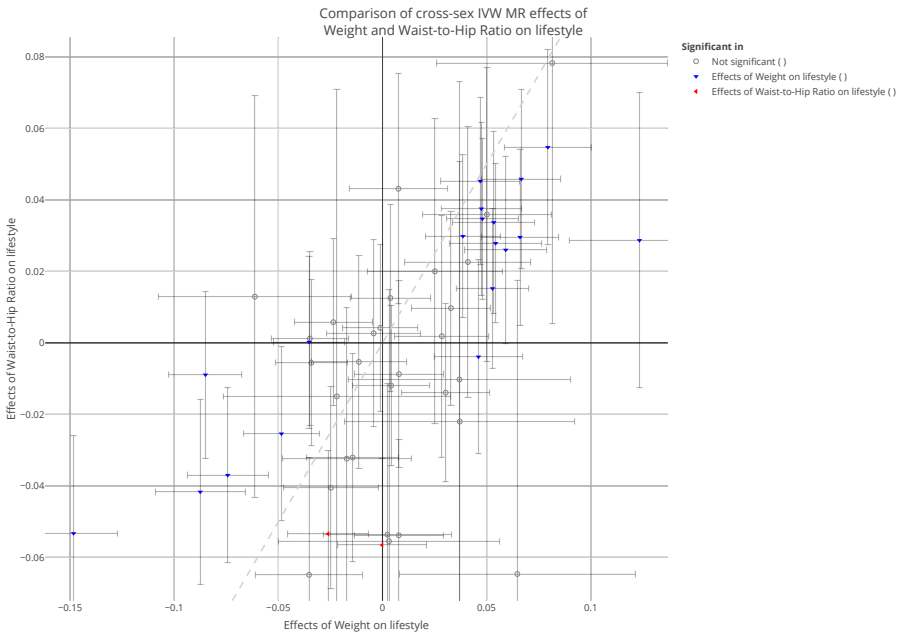

Supplementary figure 45: Comparison of effects of weight and WHR on lifestyle phenotypes estimated using cross-sex inverse-variance weighted (IVW) Mendelian randomization (MR) (X-axis) and weighted median MR (Y-axis). Each point is a distinct outcome, its coordinates showing the estimated causal effects from both methods. All summary statistics were calculated in the UK Biobank. The error bars show the 95 confidence interval.

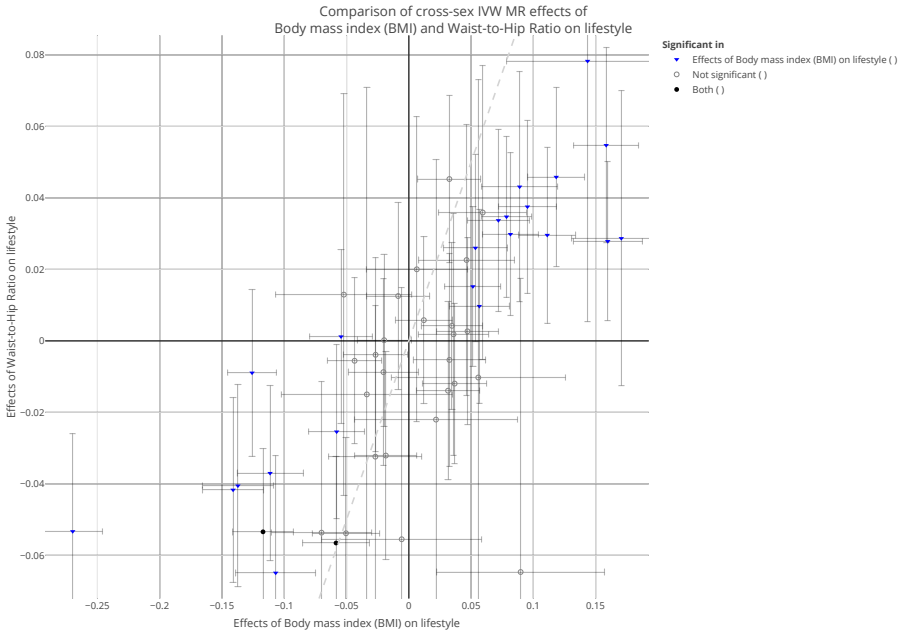

Supplementary figure 46: Comparison of effects of BMI and WHR on lifestyle phenotypes estimated using cross-sex inverse-variance weighted (IVW) Mendelian randomization (MR) (X-axis) and weighted median MR (Y-axis). Each point is a distinct outcome, its coordinates showing the estimated causal effects from both methods. All summary statistics were calculated in the UK Biobank. The error bars show the 95 confidence interval.

Supplementary Note 5: Sex-specific effects

5.1 In dietary habits

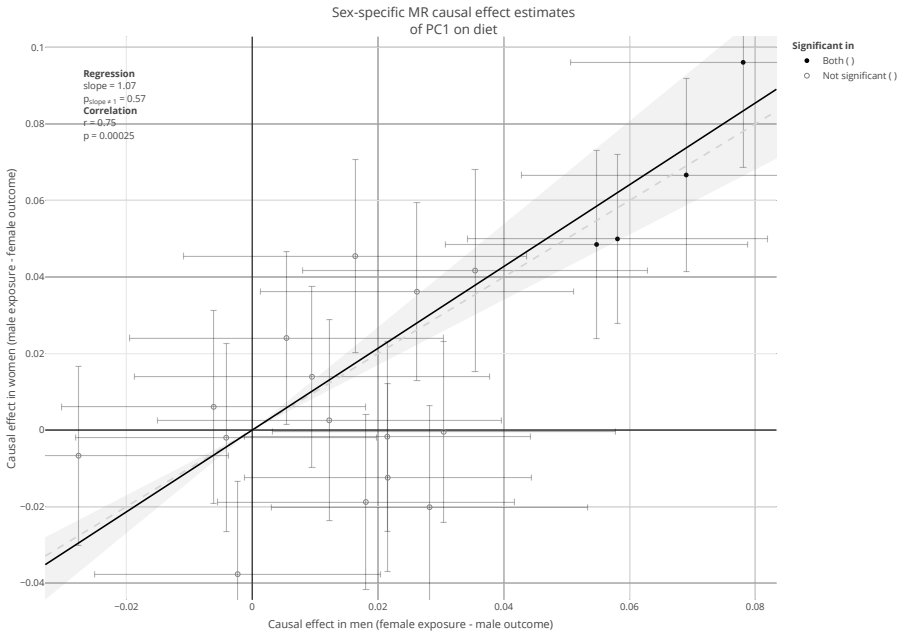

Supplementary figure 47: Comparison of sex-specific effects of PC1 on dietary habits, estimated using cross-sex inverse-variance weighted (IVW) Mendelian randomization (MR). Each point is a distinct outcome, its coordinates showing the estimated causal effects from both methods. All summary statistics were calculated in the UK Biobank. The error bars show the 95 confidence interval.

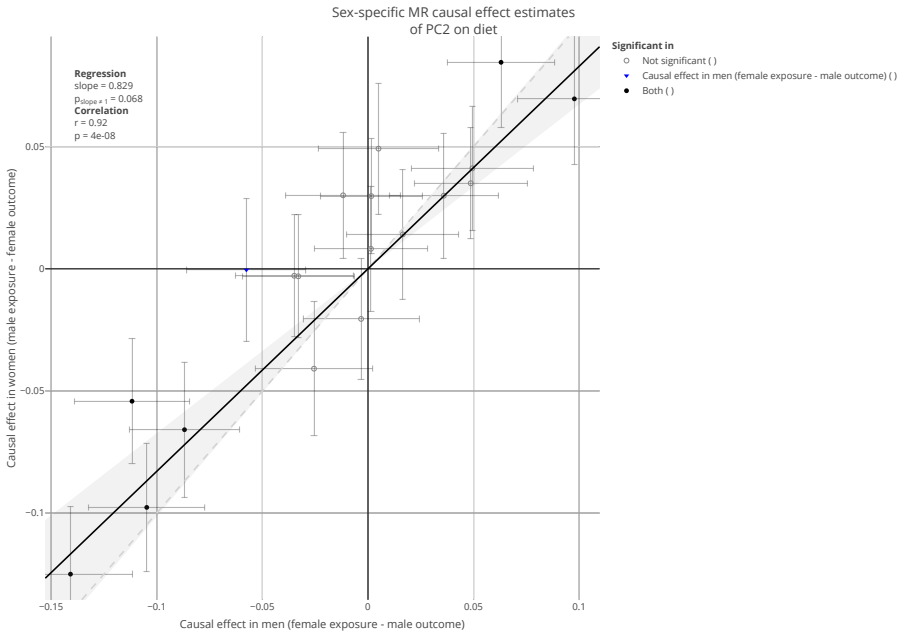

Supplementary figure 48: Comparison of sex-specific effects of PC2 on dietary habits, estimated using cross-sex inverse-variance weighted (IVW) Mendelian randomization (MR). Each point is a distinct outcome, its coordinates showing the estimated causal effects from both methods. All summary statistics were calculated in the UK Biobank. The error bars show the 95 confidence interval.

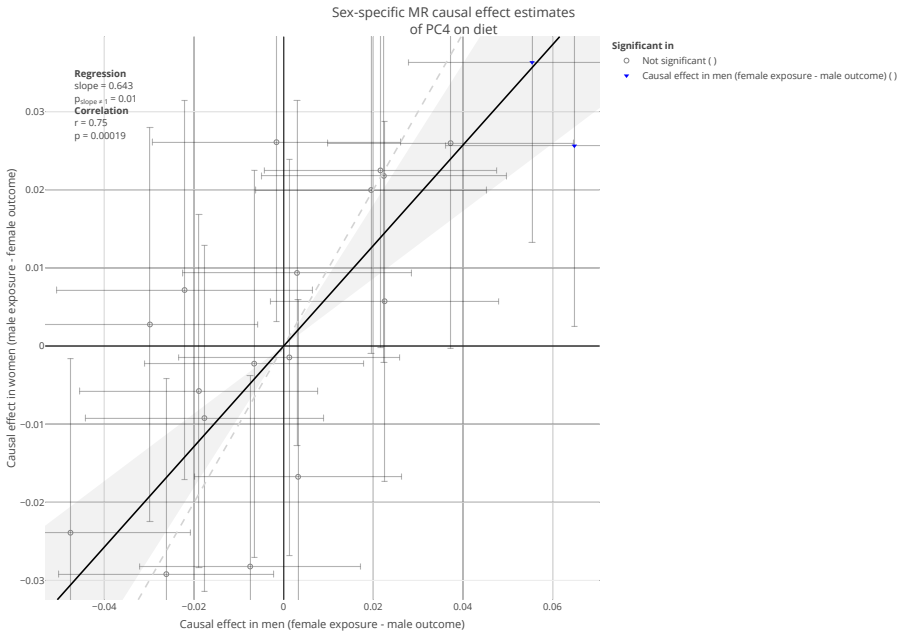

Supplementary figure 49: Comparison of sex-specific effects of PC4 on dietary habits, estimated using cross-sex inverse-variance weighted (IVW) Mendelian randomization (MR). Each point is a distinct outcome, its coordinates showing the estimated causal effects from both methods. All summary statistics were calculated in the UK Biobank. The error bars show the 95 confidence interval.

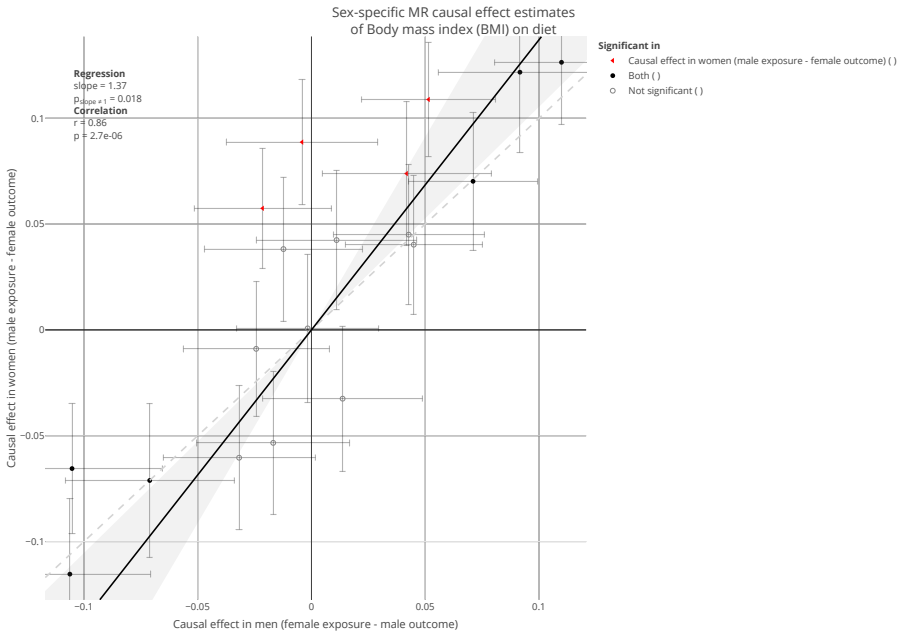

Supplementary figure 50: Comparison of sex-specific effects of BMI on dietary habits, estimated using cross-sex inverse-variance weighted (IVW) Mendelian randomization (MR). Each point is a distinct outcome, its coordinates showing the estimated causal effects from both methods. All summary statistics were calculated in the UK Biobank. The error bars show the 95 confidence interval.

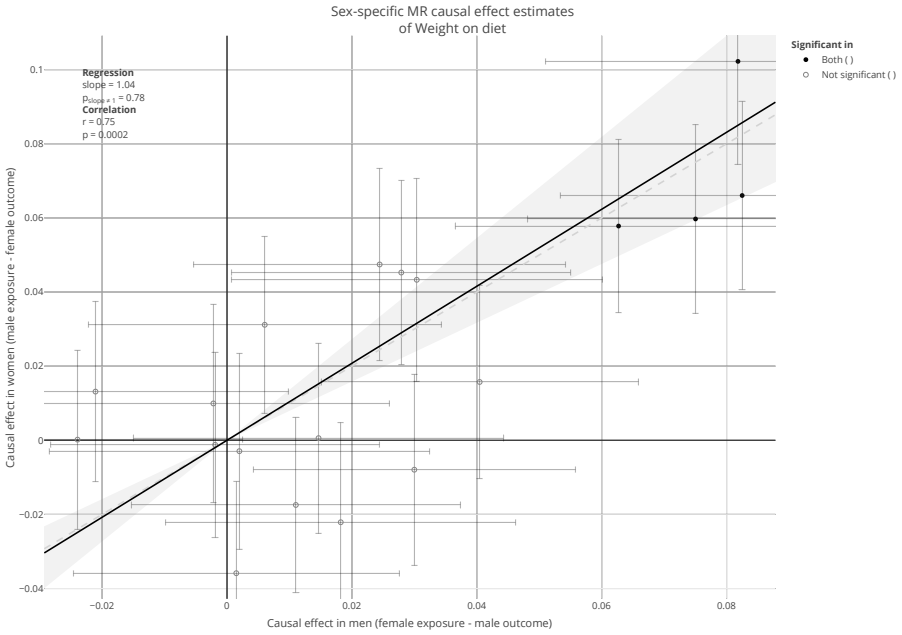

Supplementary figure 51: Comparison of sex-specific effects of weight on dietary habits, estimated using cross-sex inverse-variance weighted (IVW) Mendelian randomization (MR). Each point is a distinct outcome, its coordinates showing the estimated causal effects from both methods. All summary statistics were calculated in the UK Biobank. The error bars show the 95 confidence interval.

5.2 In diseases

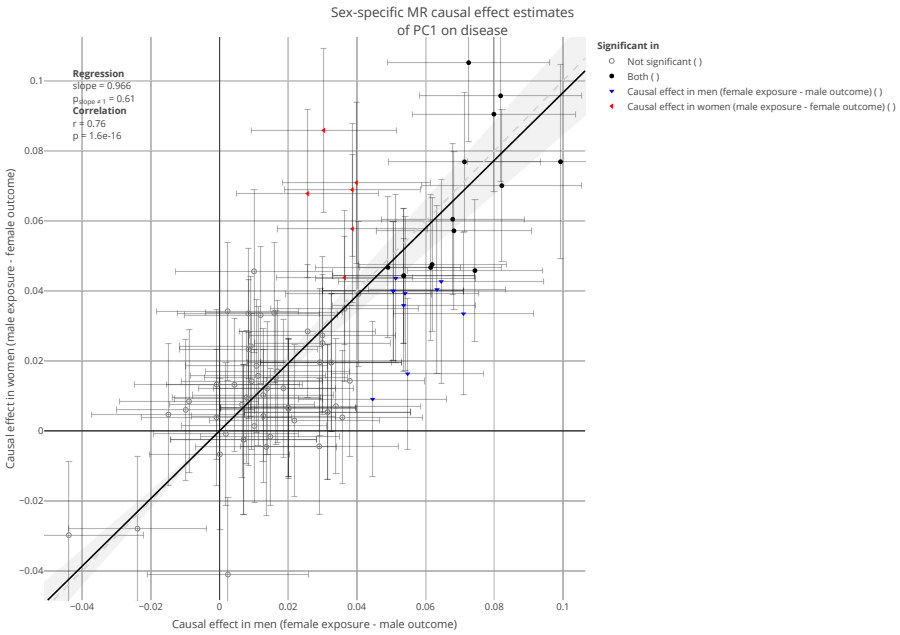

Supplementary figure 52: Comparison of sex-specific effects of PC1 on diseases, estimated using cross-sex inverse-variance weighted (IVW) Mendelian randomization (MR). Each point is a distinct outcome, its coordinates showing the estimated causal effects from both methods. All summary statistics were calculated in the UK Biobank. The error bars show the 95 confidence interval.

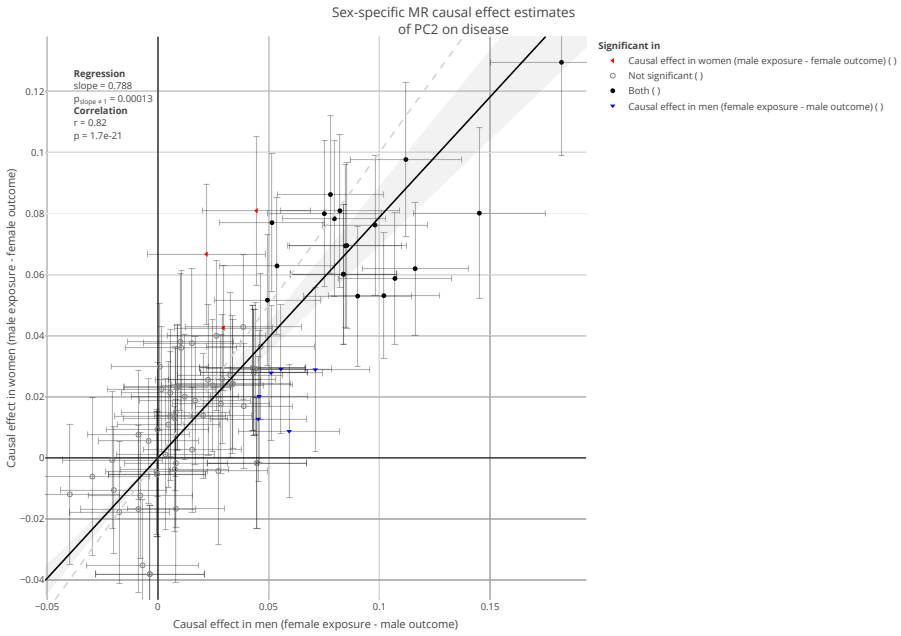

Supplementary figure 53: Comparison of sex-specific effects of PC2 on diseases, estimated using cross-sex inverse-variance weighted (IVW) Mendelian randomization (MR). Each point is a distinct outcome, its coordinates showing the estimated causal effects from both methods. All summary statistics were calculated in the UK Biobank. The error bars show the 95 confidence interval.

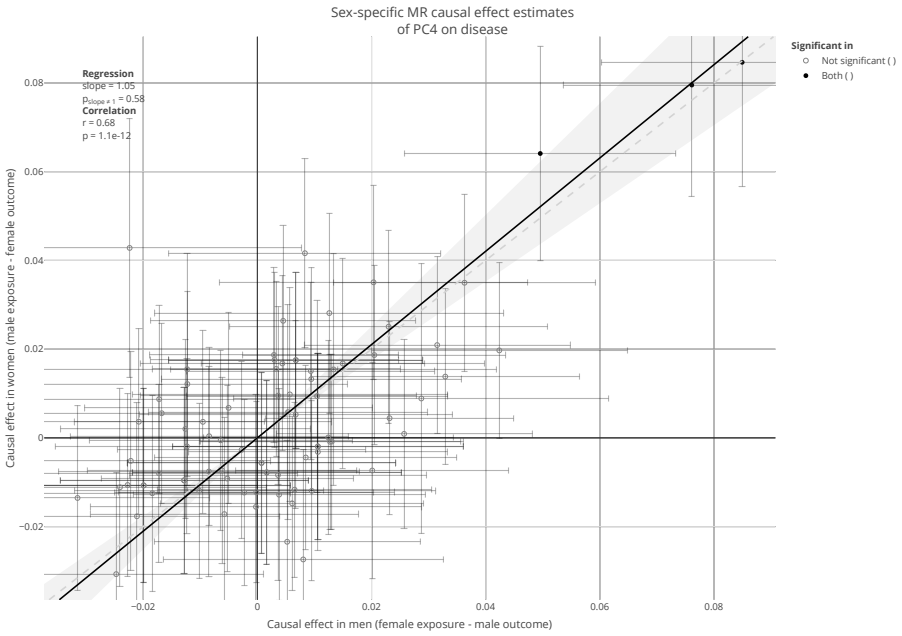

Supplementary figure 54: Comparison of sex-specific effects of PC4 on diseases, estimated using cross-sex inverse-variance weighted (IVW) Mendelian randomization (MR). Each point is a distinct outcome, its coordinates showing the estimated causal effects from both methods. All summary statistics were calculated in the UK Biobank. The error bars show the 95 confidence interval.

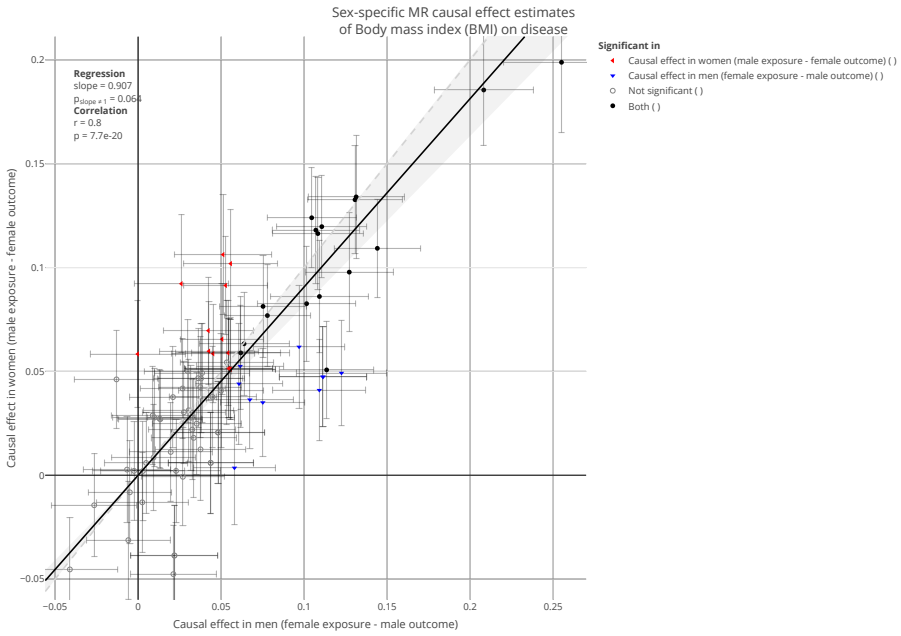

Supplementary figure 55: Comparison of sex-specific effects of BMI on diseases, estimated using cross-sex inverse-variance weighted (IVW) Mendelian randomization (MR). Each point is a distinct outcome, its coordinates showing the estimated causal effects from both methods. All summary statistics were calculated in the UK Biobank. The error bars show the 95 confidence interval.

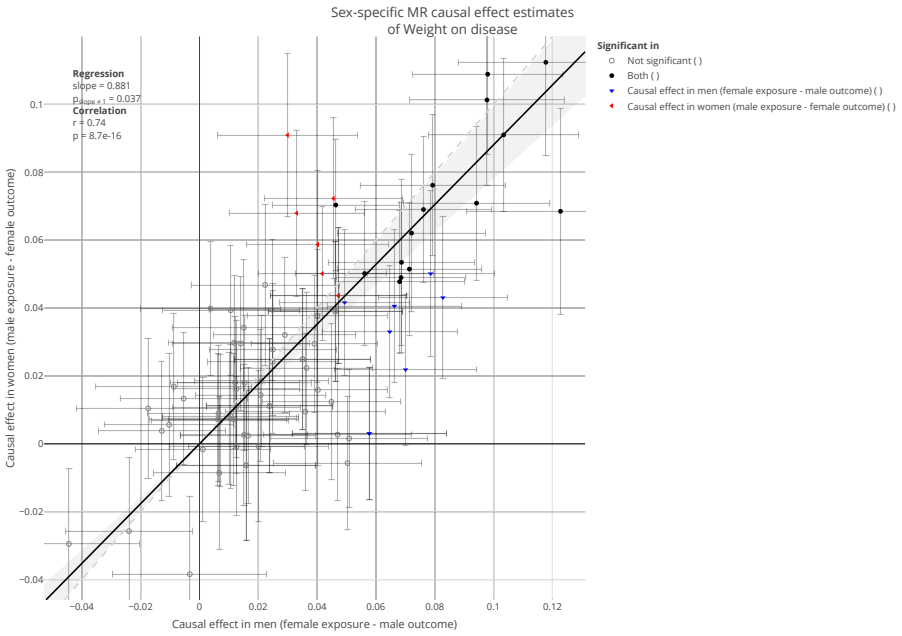

Supplementary figure 56: Comparison of sex-specific effects of weight on diseases, estimated using cross-sex inverse-variance weighted (IVW) Mendelian randomization (MR). Each point is a distinct outcome, its coordinates showing the estimated causal effects from both methods. All summary statistics were calculated in the UK Biobank. The error bars show the 95 confidence interval.

5.3 In lifestyle phenotypes

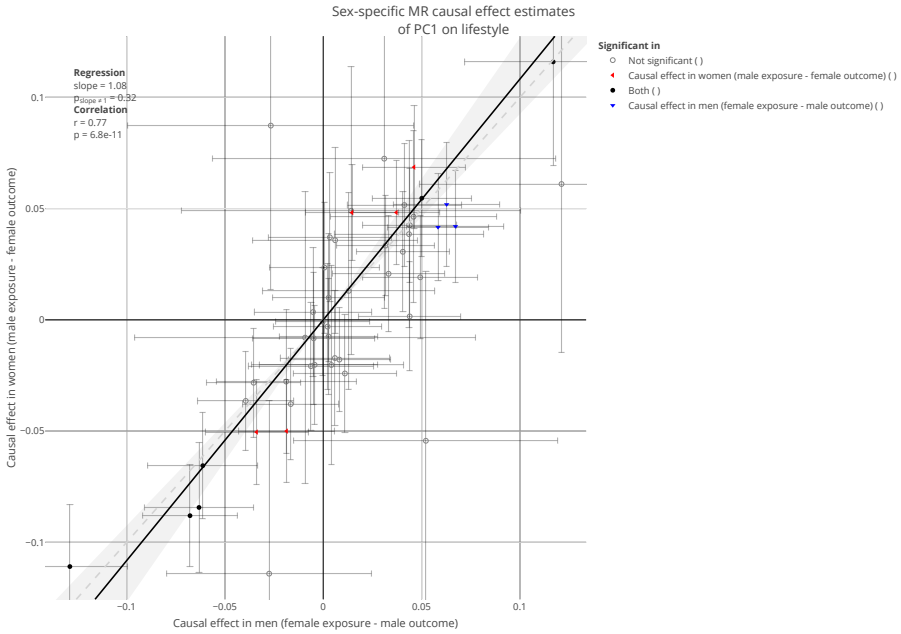

Supplementary figure 57: Comparison of sex-specific effects of PC1 on lifestyle phenotypes, estimated using cross-sex inverse-variance weighted (IVW) Mendelian randomization (MR). Each point is a distinct outcome, its coordinates showing the estimated causal effects from both methods. All summary statistics were calculated in the UK Biobank. The error bars show the 95 confidence interval.

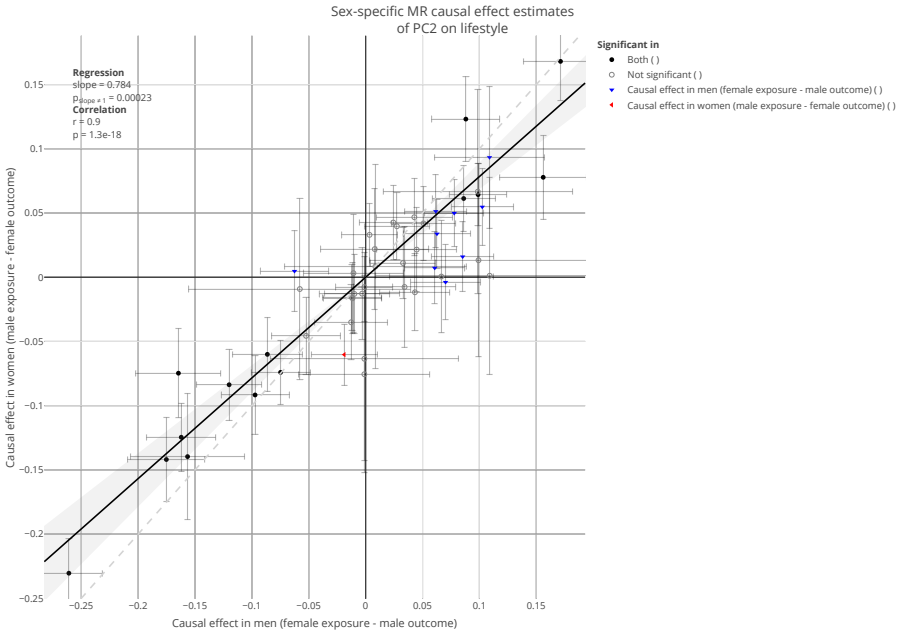

Supplementary figure 58: Comparison of sex-specific effects of PC2 on lifestyle phenotypes, estimated using cross-sex inverse-variance weighted (IVW) Mendelian randomization (MR). Each point is a distinct outcome, its coordinates showing the estimated causal effects from both methods. All summary statistics were calculated in the UK Biobank. The error bars show the 95 confidence interval.

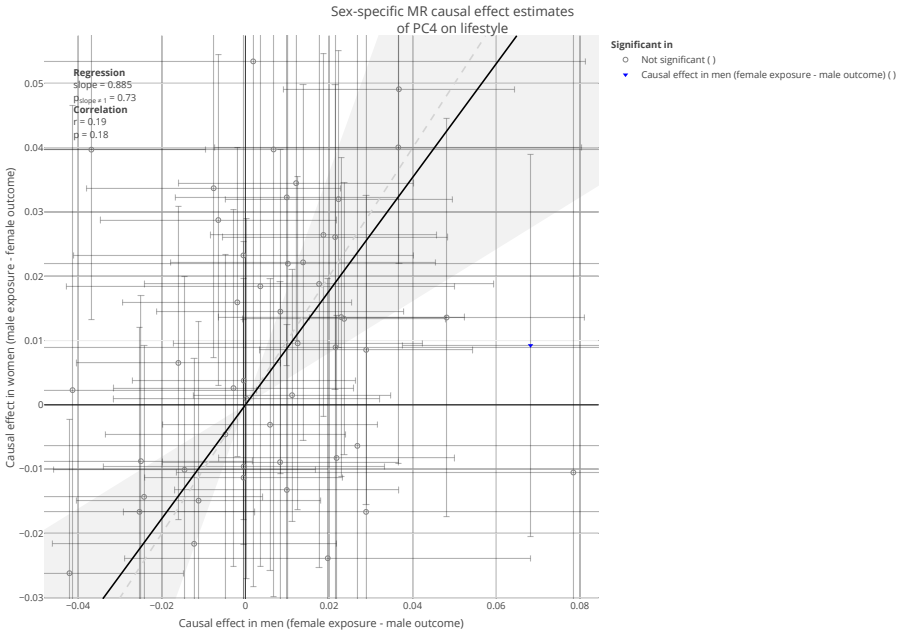

Supplementary figure 59: Comparison of sex-specific effects of PC4 on lifestyle phenotypes, estimated using cross-sex inverse-variance weighted (IVW) Mendelian randomization (MR). Each point is a distinct outcome, its coordinates showing the estimated causal effects from both methods. All summary statistics were calculated in the UK Biobank. The error bars show the 95 confidence interval.

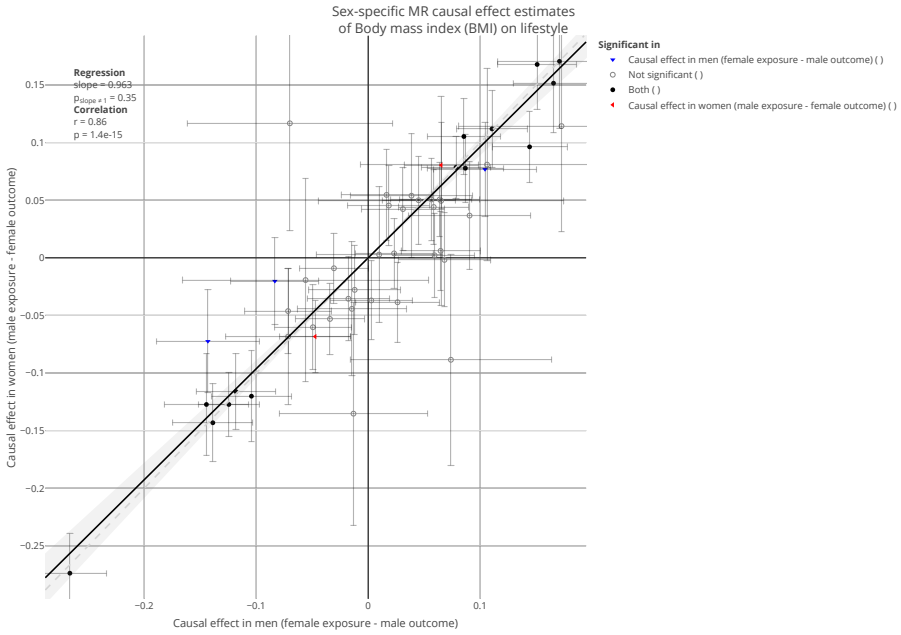

Supplementary figure 60: Comparison of sex-specific effects of BMI on lifestyle phenotypes, estimated using cross-sex inverse-variance weighted (IVW) Mendelian randomization (MR). Each point is a distinct outcome, its coordinates showing the estimated causal effects from both methods. All summary statistics were calculated in the UK Biobank. The error bars show the 95 confidence interval.

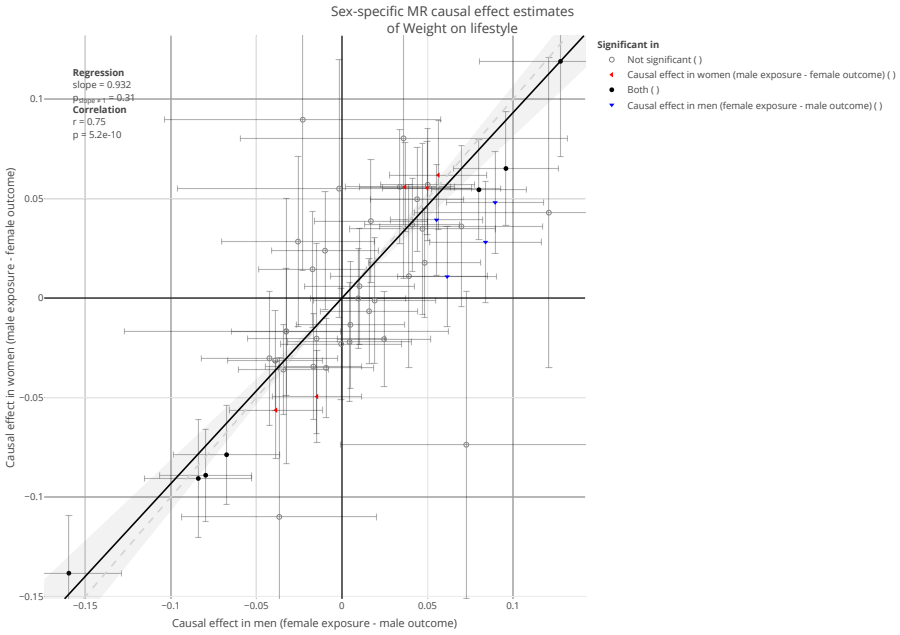

Supplementary figure 61: Comparison of sex-specific effects of weight on lifestyle phenotypes, estimated using cross-sex inverse-variance weighted (IVW) Mendelian randomization (MR). Each point is a distinct outcome, its coordinates showing the estimated causal effects from both methods. All summary statistics were calculated in the UK Biobank. The error bars show the 95 confidence interval.

5.4 In continuous measures of health

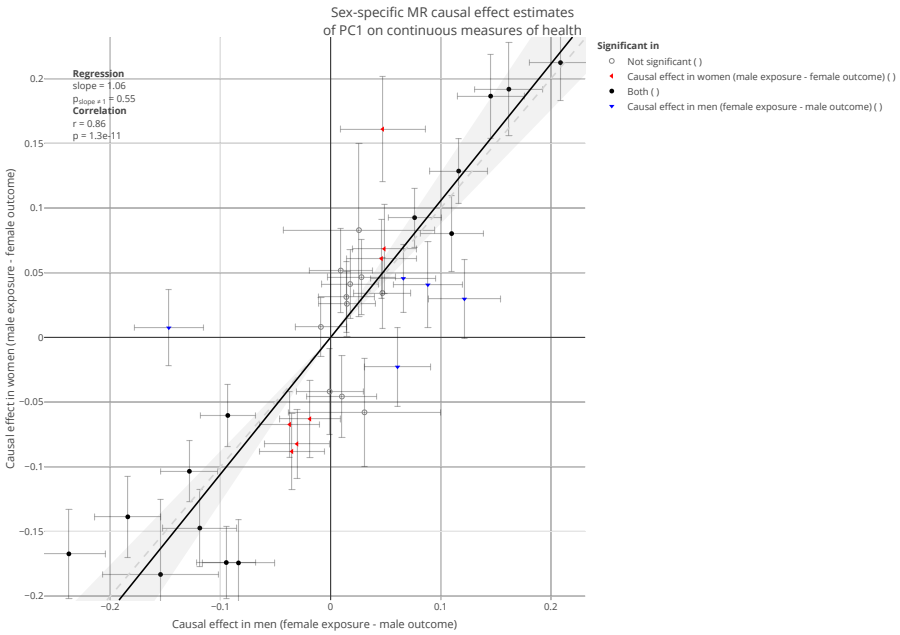

Supplementary figure 62: Comparison of sex-specific effects of PC1 on continuous measures of health, estimated using cross-sex inverse-variance weighted (IVW) Mendelian randomization (MR). Each point is a distinct outcome, its coordinates showing the estimated causal effects from both methods. All summary statistics were calculated in the UK Biobank. The error bars show the 95 confidence interval.

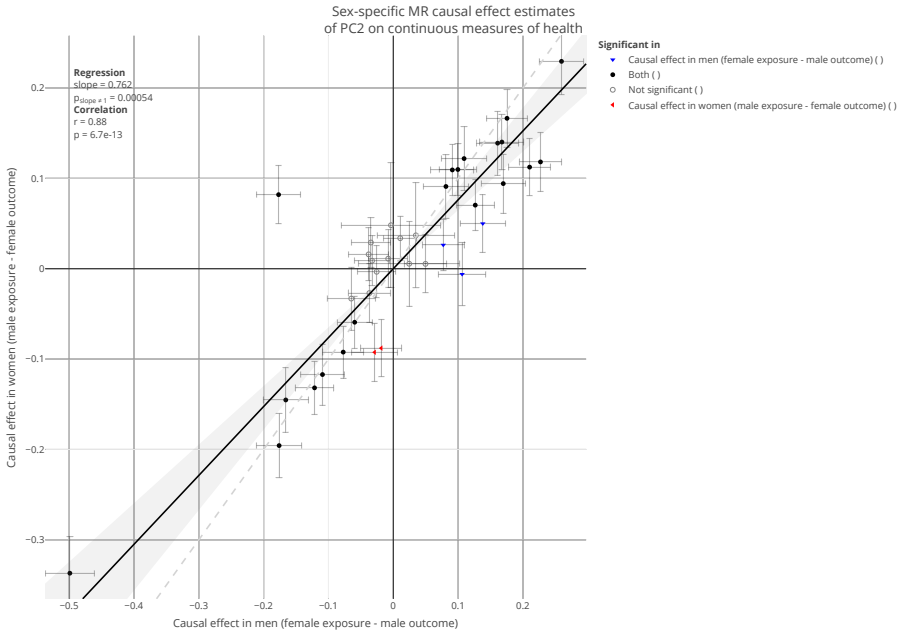

Supplementary figure 63: Comparison of sex-specific effects of PC2 on continuous measures of health, estimated using cross-sex inverse-variance weighted (IVW) Mendelian randomization (MR). Each point is a distinct outcome, its coordinates showing the estimated causal effects from both methods. All summary statistics were calculated in the UK Biobank. The error bars show the 95 confidence interval.

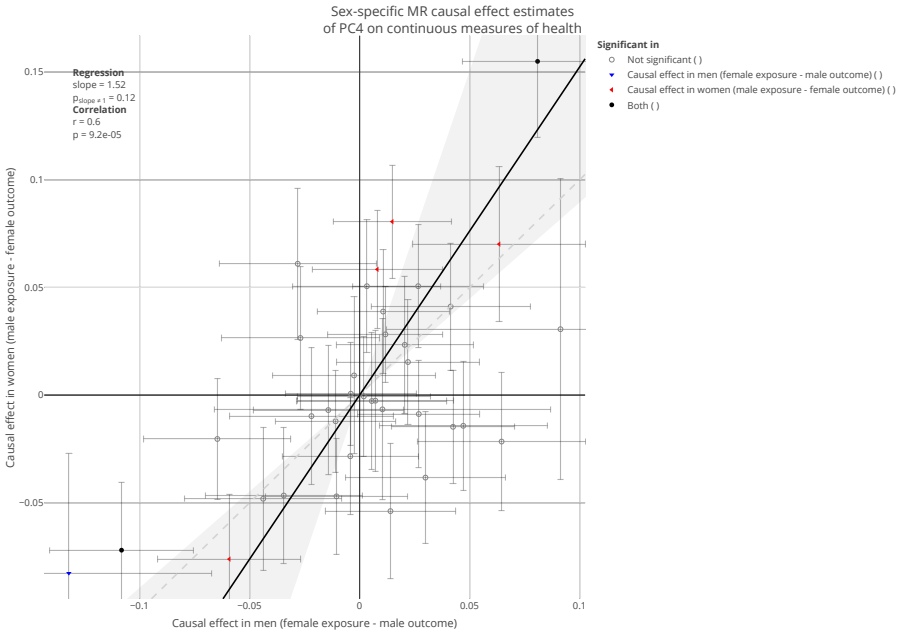

Supplementary figure 64: Comparison of sex-specific effects of PC4 on continuous measures of health, estimated using cross-sex inverse-variance weighted (IVW) Mendelian randomization (MR). Each point is a distinct outcome, its coordinates showing the estimated causal effects from both methods. All summary statistics were calculated in the UK Biobank. The error bars show the 95 confidence interval.

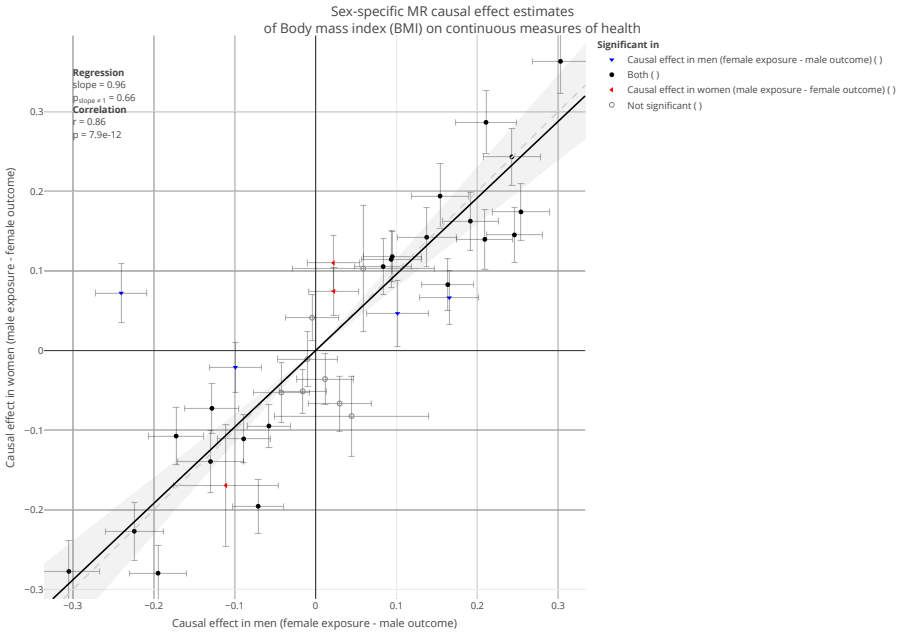

Supplementary figure 65: Comparison of sex-specific effects of BMI on continuous measures of health, estimated using cross-sex inverse-variance weighted (IVW) Mendelian randomization (MR). Each point is a distinct outcome, its coordinates showing the estimated causal effects from both methods. All summary statistics were calculated in the UK Biobank. The error bars show the 95 confidence interval.

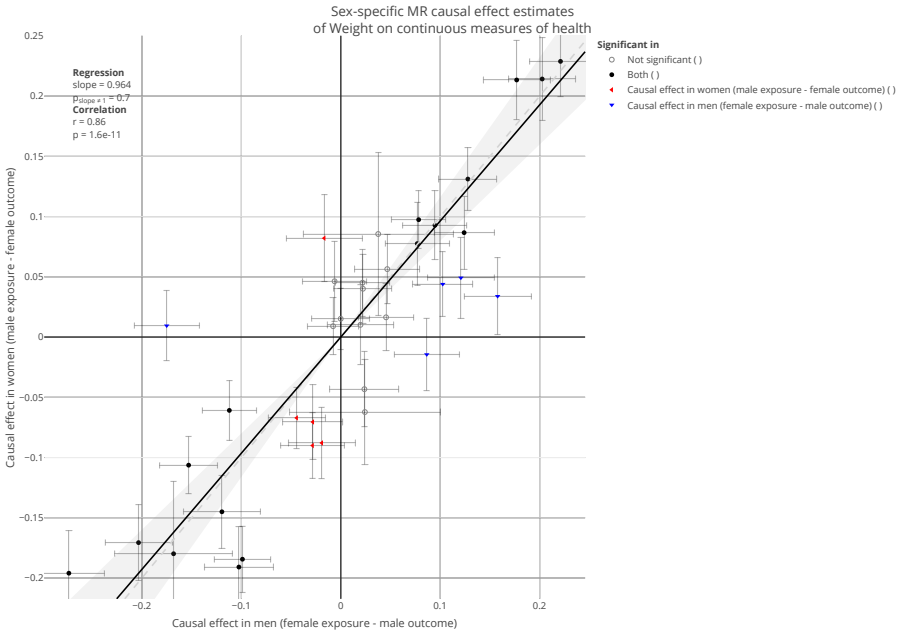

Supplementary figure 66: Comparison of sex-specific effects of weight on continuous measures of health, estimated using cross-sex inverse-variance weighted (IVW) Mendelian randomization (MR). Each point is a distinct outcome, its coordinates showing the estimated causal effects from both methods. All summary statistics were calculated in the UK Biobank. The error bars show the 95 confidence interval.

Supplementary Note 6: Disease prediction

6.1 Within-sample

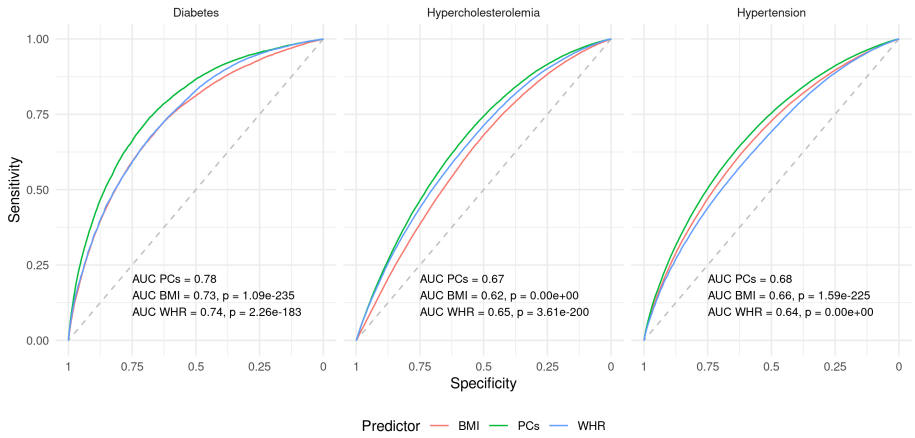

Supplementary figure 67: ROC curves for within-sample PC-, BMI-, and WHR-based prediction of diabetes, hypercholesterolemia, and hypertension. The indicated p-values for the difference between the PC- and single trait-based curves were obtained using the DeLong method.

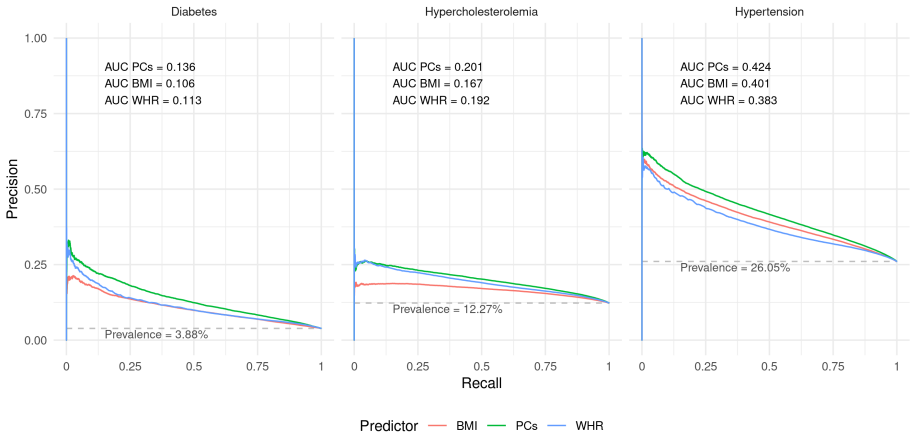

Supplementary figure 68: Precision-Recall curves for within-sample PC-, BMI-, and WHR-based prediction of diabetes, hypercholesterolemia, and hypertension.

6.2 Out-of-sample/population

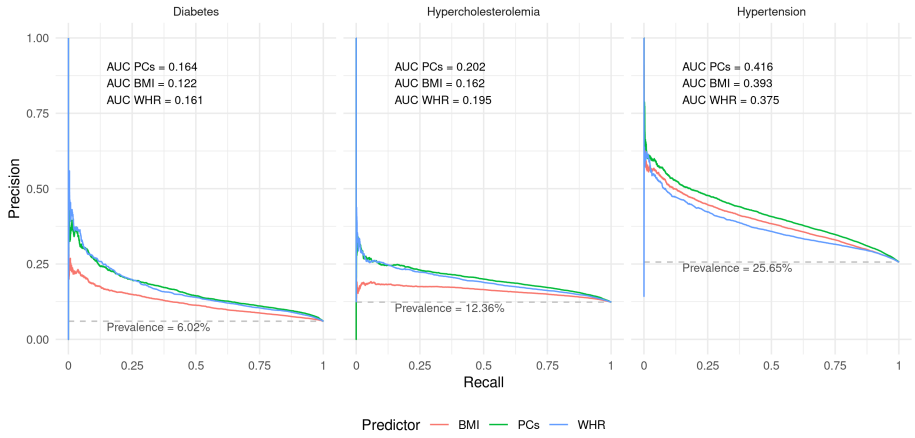

Supplementary figure 69: Precision-Recall curves for out-of-sample/population PC-, BMI-, and WHR-based prediction of diabetes, hypercholesterolemia, and hypertension.

Supplementary Note 7: Robustness of causal effect estimates for low prevalence diseases

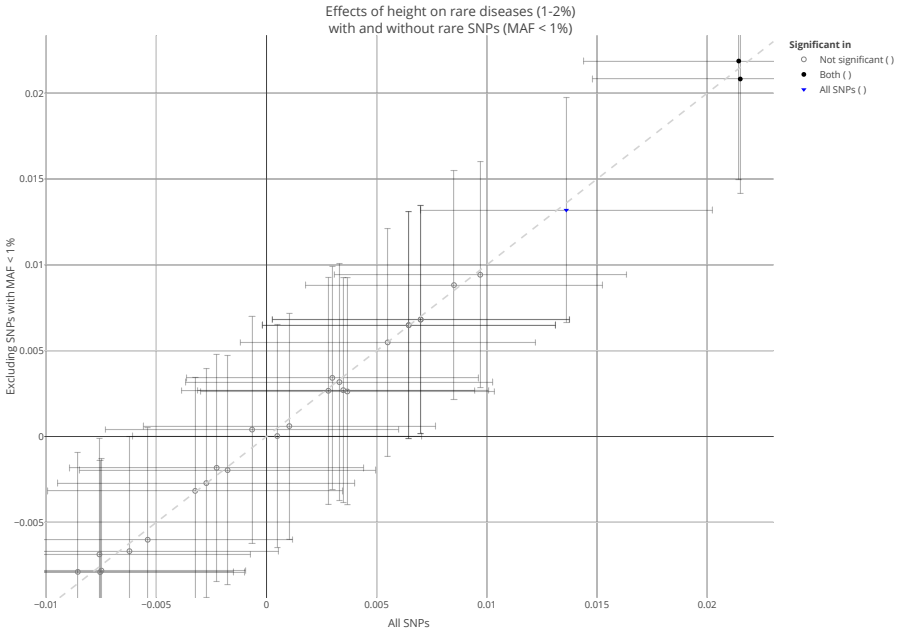

Supplementary figure 70: Comparison of estimates for the causal effect of standing height on diseases with low prevalence (1-2%), using all IVs (X-axis) or excluding SNPs with a MAF $< 1\%$ (comprising 88 of 1704 SNPs, Y-axis). Each point is a distinct outcome, its coordinates showing the estimated causal effects from both sets of IVs. All summary statistics were calculated in the UK Biobank. The error bars show the 95 confidence interval.

Supplementary Note 8: Cross-sex vs. standard MR in a single sample

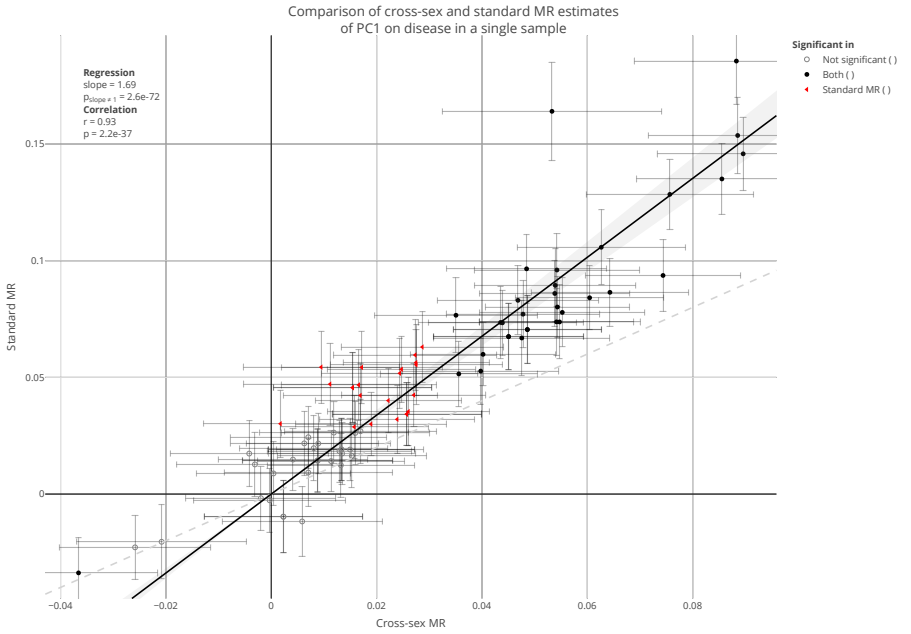

Supplementary figure 71: Comparison of effects of PC1 on disease estimated using cross-sex inverse-variance weighted (IVW) Mendelian randomization (MR) (X-axis) and standard IVW MR (Y-axis). Each point is a distinct outcome, its coordinates showing the estimated causal effects from both methods. All summary statistics were calculated in the UK Biobank. The error bars show the 95 confidence interval.

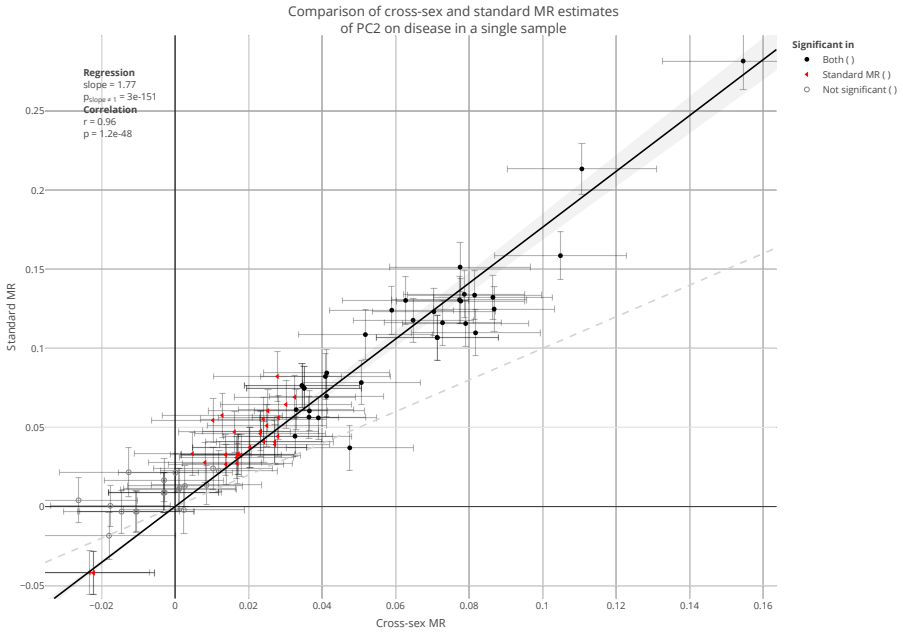

Supplementary figure 72: Comparison of effects of PC2 on disease estimated using cross-sex inverse-variance weighted (IVW) Mendelian randomization (MR) (X-axis) and standard IVW MR (Y-axis). Each point is a distinct outcome, its coordinates showing the estimated causal effects from both methods. All summary statistics were calculated in the UK Biobank. The error bars show the 95 confidence interval.

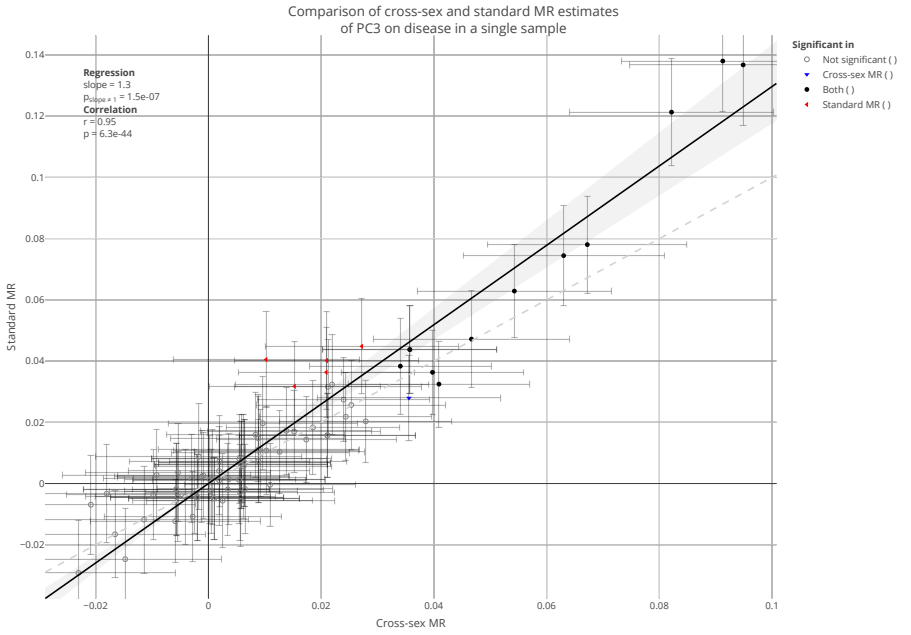

Supplementary figure 73: Comparison of effects of PC3 on disease estimated using cross-sex inverse-variance weighted (IVW) Mendelian randomization (MR) (X-axis) and standard IVW MR (Y-axis). Each point is a distinct outcome, its coordinates showing the estimated causal effects from both methods. All summary statistics were calculated in the UK Biobank. The error bars show the 95 confidence interval.

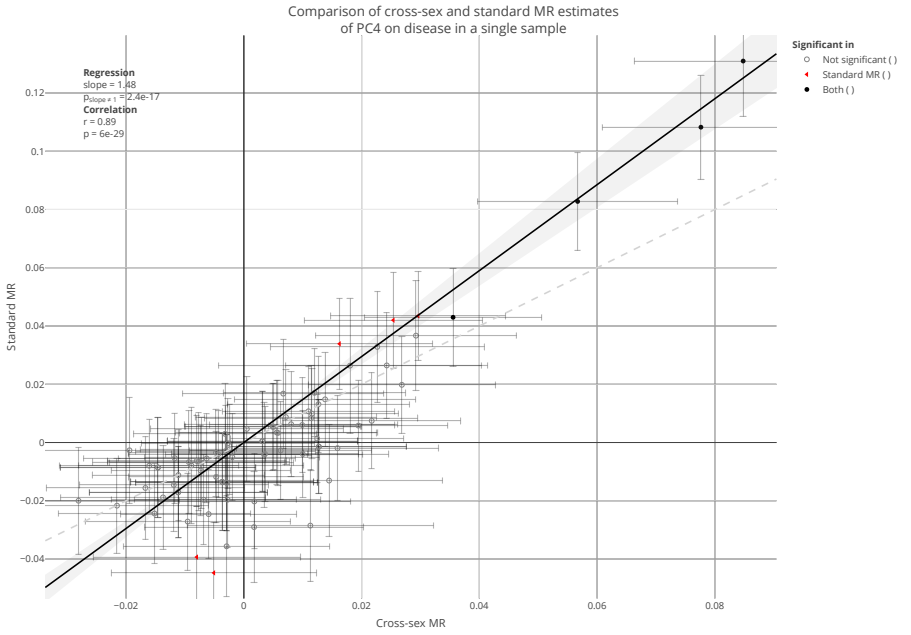

Supplementary figure 74: Comparison of effects of PC4 on disease estimated using cross-sex inverse-variance weighted (IVW) Mendelian randomization (MR) (X-axis) and standard IVW MR (Y-axis). Each point is a distinct outcome, its coordinates showing the estimated causal effects from both methods. All summary statistics were calculated in the UK Biobank. The error bars show the 95 confidence interval.

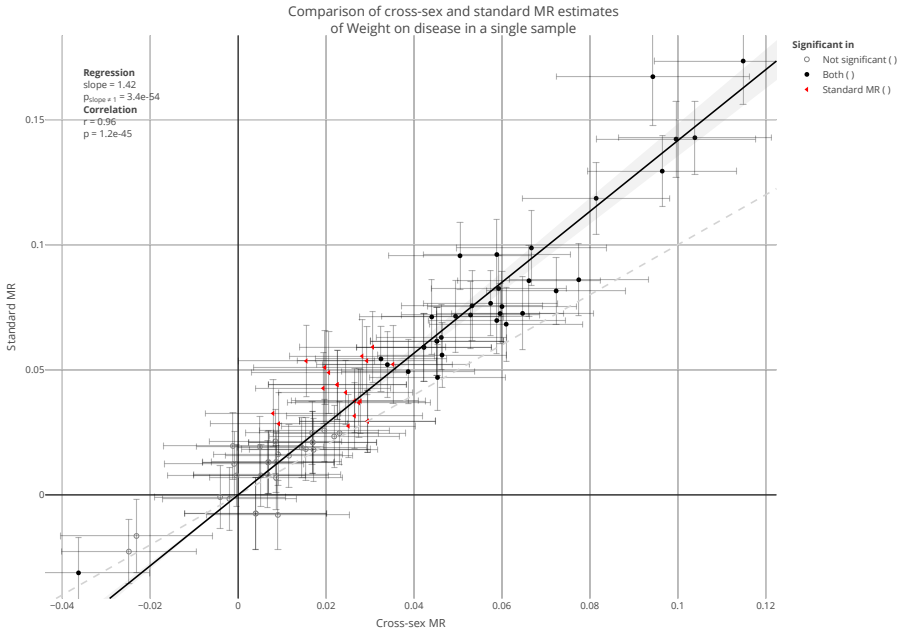

Supplementary figure 75: Comparison of effects of weight on disease estimated using cross-sex inverse-variance weighted (IVW) Mendelian randomization (MR) (X-axis) and standard IVW MR (Y-axis). Each point is a distinct outcome, its coordinates showing the estimated causal effects from both methods. All summary statistics were calculated in the UK Biobank. The error bars show the 95 confidence interval.

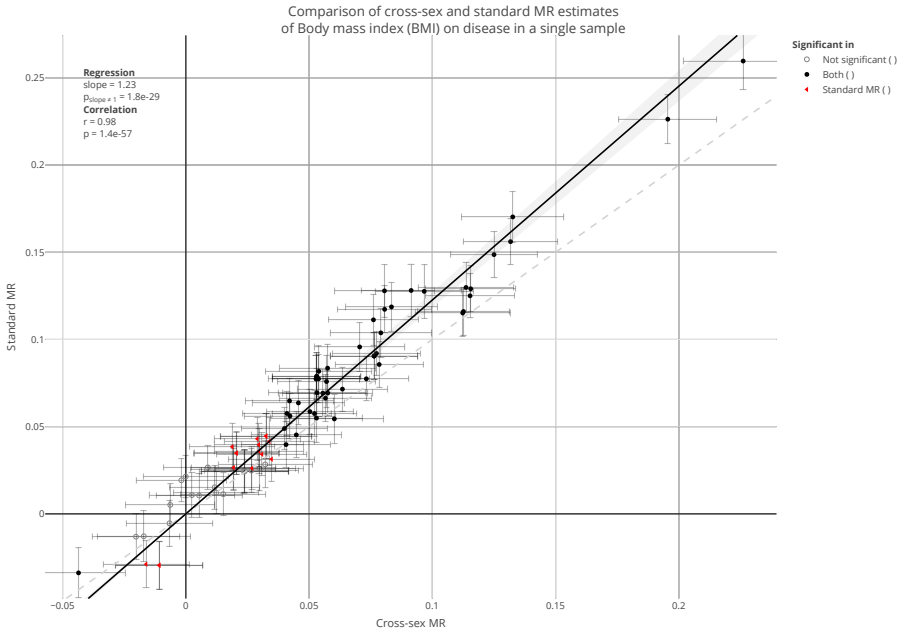

Supplementary figure 76: Comparison of effects of BMI on disease estimated using cross-sex inverse-variance weighted (IVW) Mendelian randomization (MR) (X-axis) and standard IVW MR (Y-axis). Each point is a distinct outcome, its coordinates showing the estimated causal effects from both methods. All summary statistics were calculated in the UK Biobank. The error bars show the 95 confidence interval.

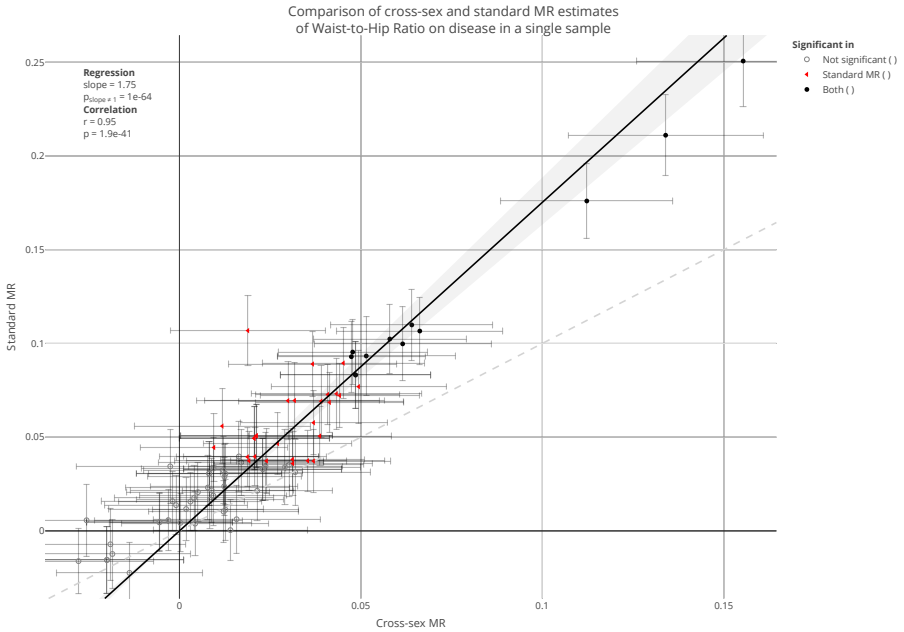

Supplementary figure 77: Comparison of effects of WHR on disease estimated using cross-sex inverse-variance weighted (IVW) Mendelian randomization (MR) (X-axis) and standard IVW MR (Y-axis). Each point is a distinct outcome, its coordinates showing the estimated causal effects from both methods. All summary statistics were calculated in the UK Biobank. The error bars show the 95 confidence interval.

Supplementary Note 9: Cross-sex vs. standard MR in two samples

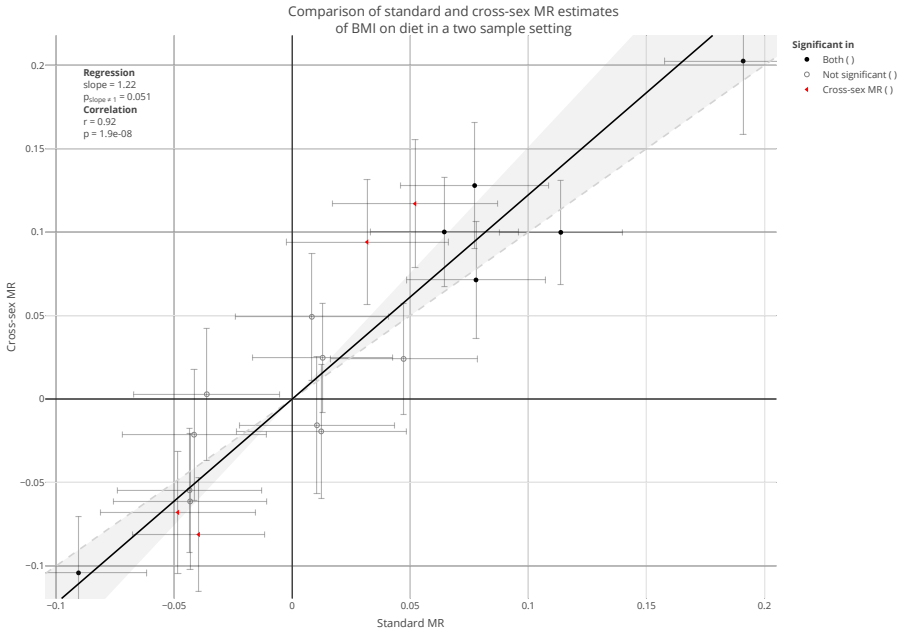

Supplementary figure 78: Comparison of effects of BMI on phenotypes related to dietary habits estimated using standard inverse-variance weighted (IVW) Mendelian randomization (MR) (X-axis) and cross-sex IVW MR (Y-axis). Each point is a distinct outcome, its coordinates showing the estimated causal effects from both methods. Summary statistics for BMI were taken from the GIANT consortium, while those for the outcomes were taken from the UK Biobank. The error bars show the 95 confidence interval.

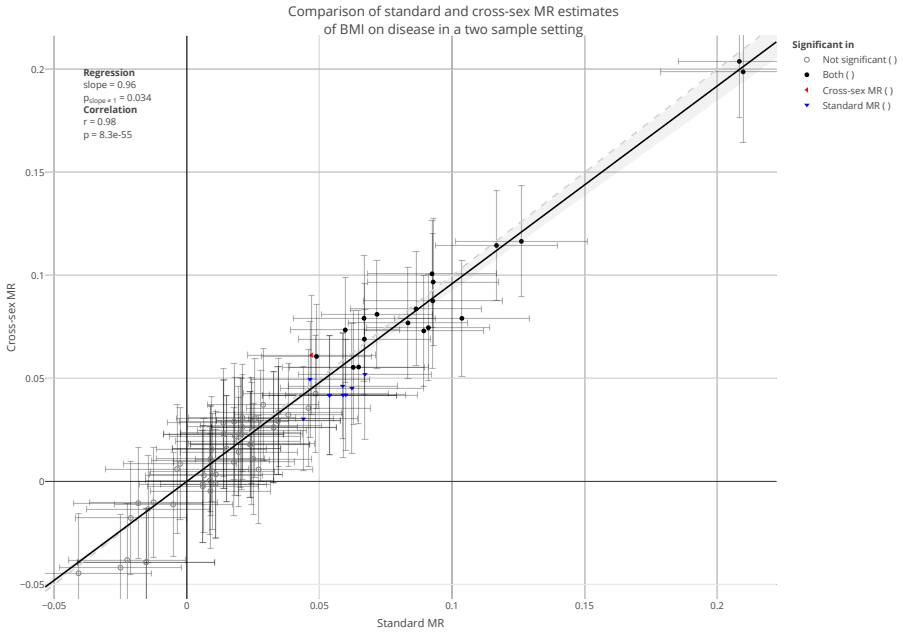

Supplementary figure 79: Comparison of effects of BMI on phenotypes related to diseases estimated using standard inverse-variance weighted (IVW) Mendelian randomization (MR) (X-axis) and cross-sex IVW MR (Y-axis). Each point is a distinct outcome, its coordinates showing the estimated causal effects from both methods. Summary statistics for BMI were taken from the GIANT consortium, while those for the outcomes were taken from the UK Biobank. The error bars show the 95 confidence interval.

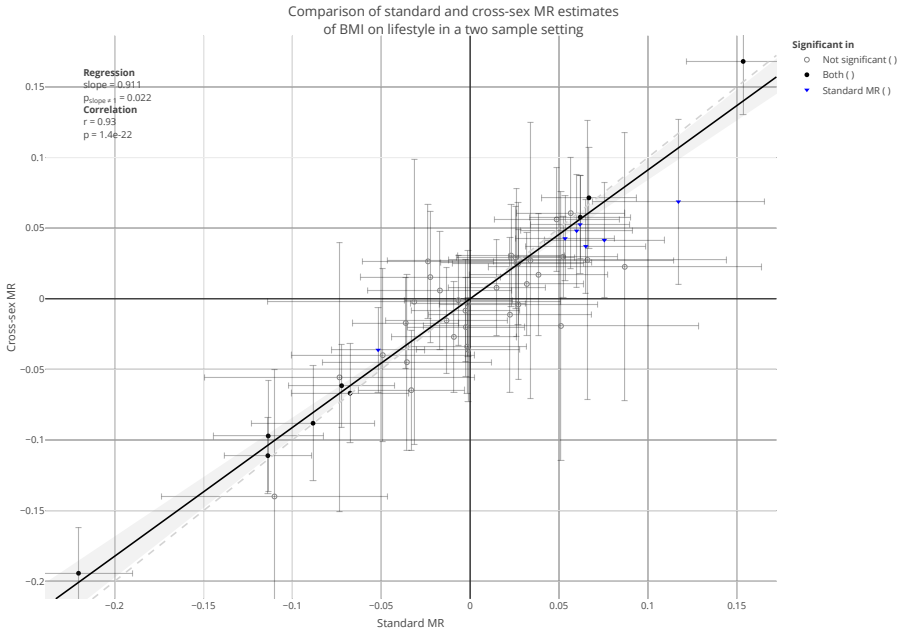

Supplementary figure 80: Comparison of effects of BMI on phenotypes related to lifestyle phenotypes estimated using standard inverse-variance weighted (IVW) Mendelian randomization (MR) (X-axis) and cross-sex IVW MR (Y-axis). Each point is a distinct outcome, its coordinates showing the estimated causal effects from both methods. Summary statistics for BMI were taken from the GIANT consortium, while those for the outcomes were taken from the UK Biobank. The error bars show the 95 confidence interval.

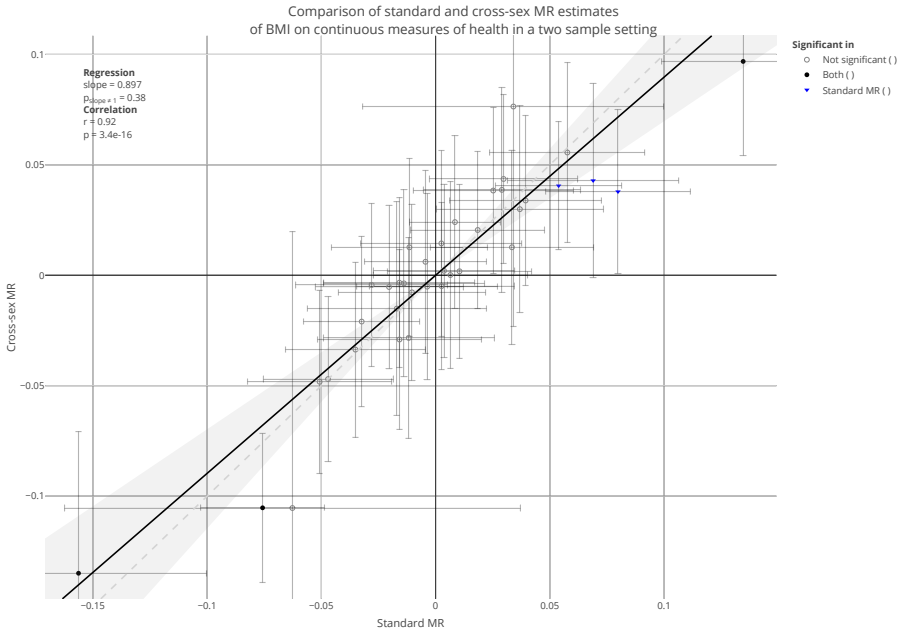

Supplementary figure 81: Comparison of effects of BMI on phenotypes related to continuous measures of health estimated using standard inverse-variance weighted (IVW) Mendelian randomization (MR) (X-axis) and cross-sex IVW MR (Y-axis). Each point is a distinct outcome, its coordinates showing the estimated causal effects from both methods. Summary statistics for BMI were taken from the GIANT consortium, while those for the outcomes were taken from the UK Biobank. The error bars show the 95 confidence interval.

Supplementary Note 10: Heterogeneity filtering alternatives

10.1 No heterogeneity filtering

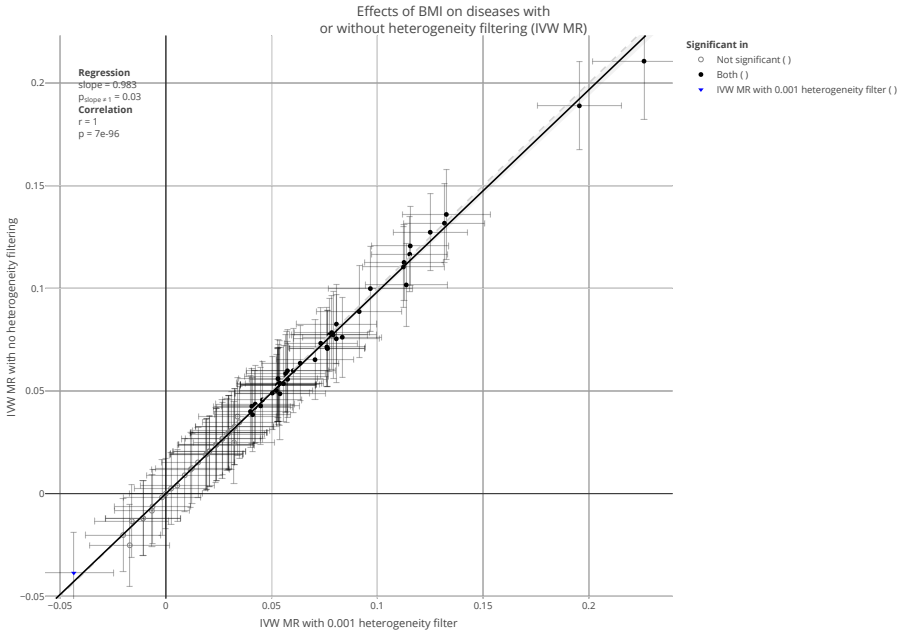

Supplementary figure 82: Comparison of estimates for the causal effect of BMI on disease using IVW MR with or without heterogeneity filtering with a p-value threshold of 0.001. Each point is a distinct outcome, its coordinates showing the estimated causal effects from both methods. All summary statistics were calculated in the UK Biobank. The error bars show the 95 confidence interval.

10.2 Weighted median MR

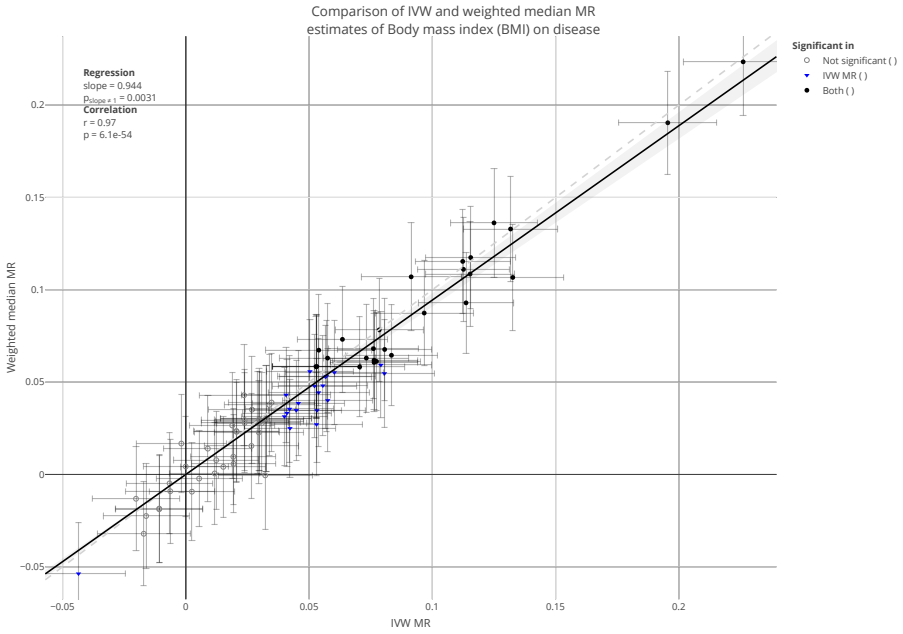

Supplementary figure 83: Comparison of estimates for the causal effects of BMI on diseases using IVW MR (X-axis) and weighted median MR (Y-axis), both with heterogeneity filtering (p-value threshold of 0.001). Each point is a distinct outcome, its coordinates showing the estimated causal effects from both methods. All summary statistics were calculated in the UK Biobank. The error bars show the 95 confidence interval.

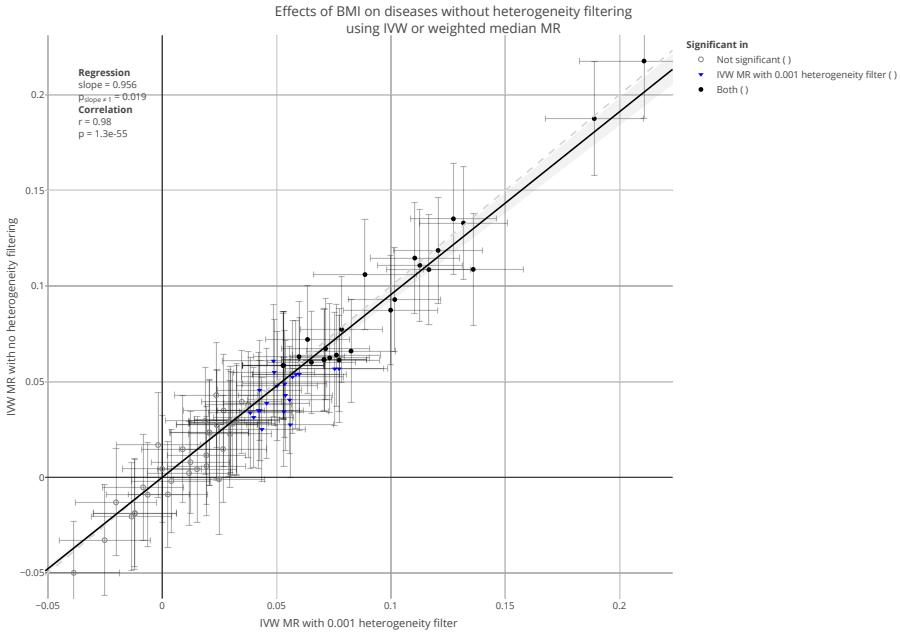

Supplementary figure 84: Comparison of estimates for the causal effect of BMI on disease using IVW or weighted median MR, both without heterogeneity filtering. Each point is a distinct outcome, its coordinates showing the estimated causal effects from both methods. All summary statistics were calculated in the UK Biobank. The error bars show the 95 confidence interval.

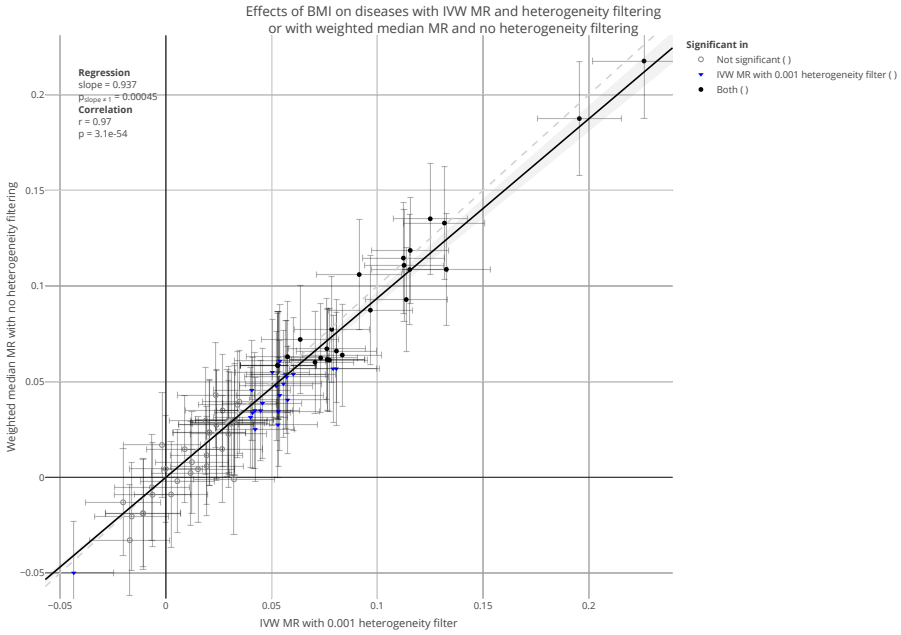

Supplementary figure 85: Comparison of estimates for the causal effect of BMI on diseases using IVW MR with heterogeneity filtering (p-value threshold of 0.001) or weighted median without heterogeneity filtering. Each point is a distinct outcome, its coordinates showing the estimated causal effects from both methods. All summary statistics were calculated in the UK Biobank. The error bars show the 95 confidence interval.

10.3 Cochran's Q vs. exact Q statistic

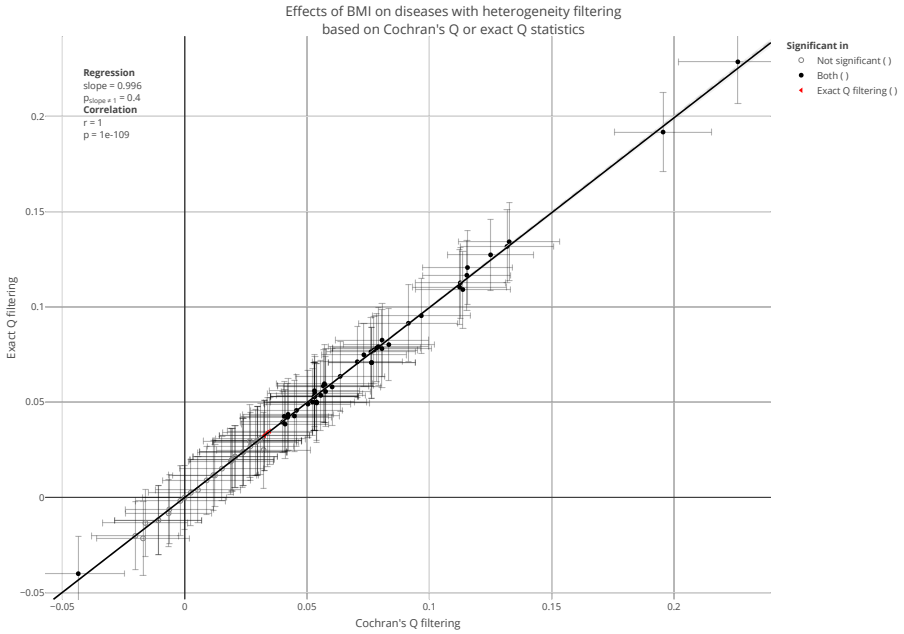

Supplementary figure 86: Comparison of estimates for the causal effect of BMI on disease, using exact Q vs. Cochran's Q statistics with a p-value threshold of 0.001. Each point is a distinct outcome, its coordinates showing the estimated causal effects from both methods. All summary statistics were calculated in the UK Biobank. The error bars show the 95 confidence interval.

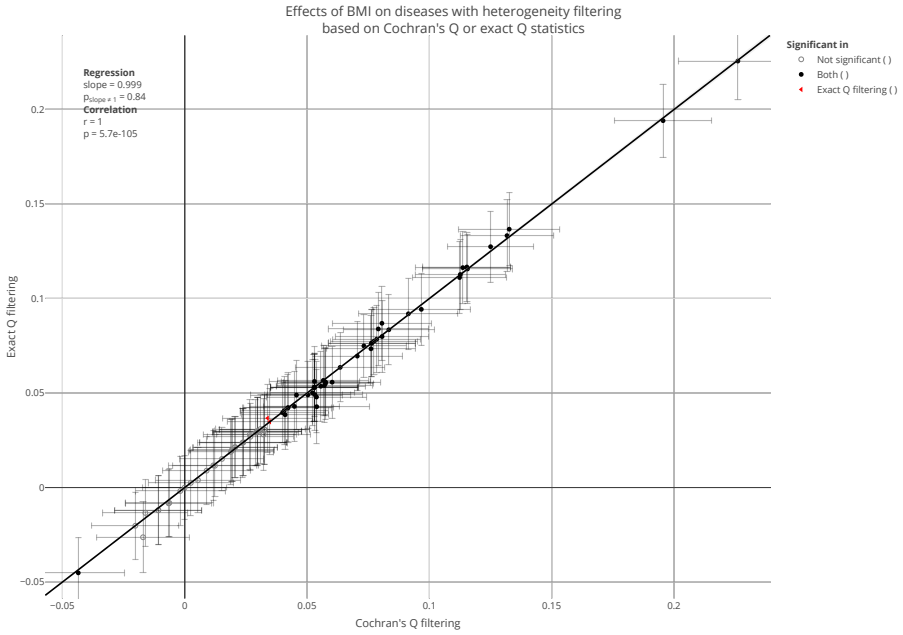

Supplementary figure 87: Comparison of estimates for the causal effect of BMI on disease, using exact Q ($p < 0.001$) vs. Cochran's Q statistics ($p < 0.05$). Each point is a distinct outcome, its coordinates showing the estimated causal effects from both methods. All summary statistics were calculated in the UK Biobank. The error bars show the 95 confidence interval.

Supplementary Note 11: Sex-specific estimates, IVW vs. cross-sex MR

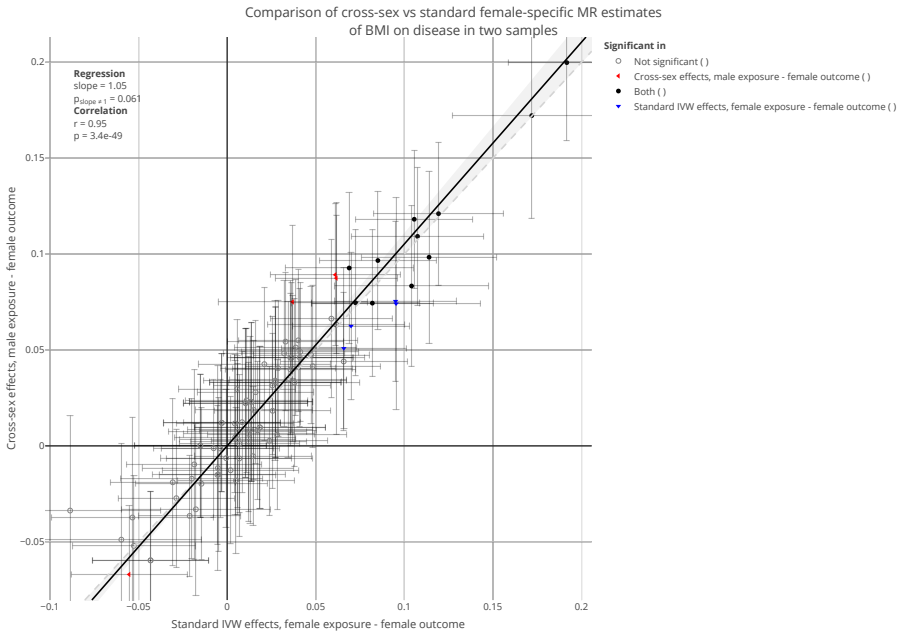

Supplementary figure 88: Comparison of female-specific effects of BMI on diseases, estimated using standard inverse-variance weighted (IVW) Mendelian randomization (MR) (X-axis, female-specific summary statistics for both exposure and outcome) and cross-sex IVW MR (Y-axis, male-specific summary statistics for exposure but female-specific ones for outcome). Each point is a distinct outcome phenotype, its coordinates showing the estimated causal effects from both methods. Summary statistics for BMI were taken from the GIANT consortium, while those for the outcomes were taken from the UK Biobank. The error bars show the 95 confidence interval.

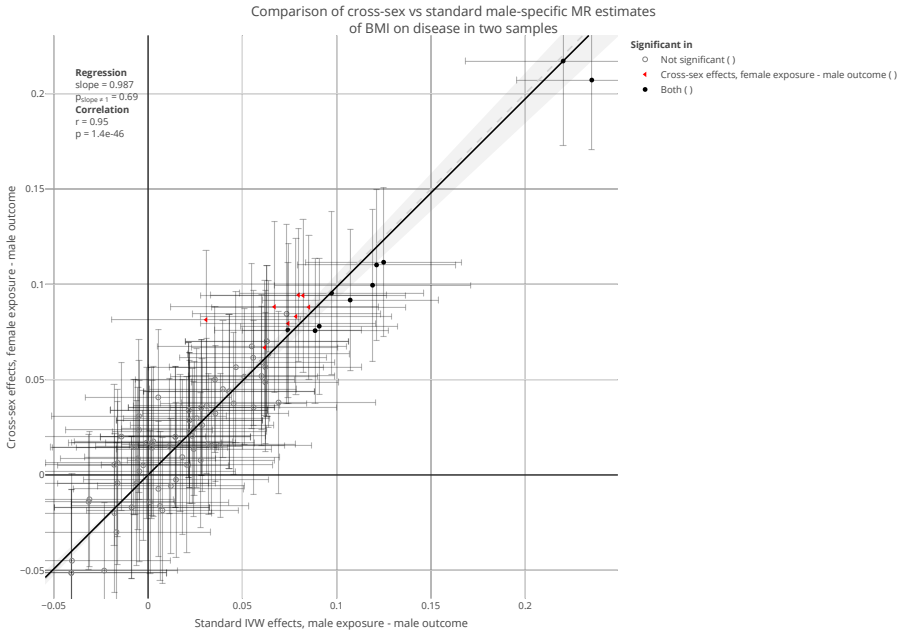

Supplementary figure 89: Comparison of male-specific effects of BMI on diseases, estimated using standard inverse-variance weighted (IVW) Mendelian randomization (MR) (X-axis, male-specific summary statistics for both exposure and outcome) and cross-sex IVW MR (Y-axis, female-specific summary statistics for exposure but male-specific ones for outcome). Each point is a distinct outcome phenotype, its coordinates showing the estimated causal effects from both methods. Summary statistics for BMI were taken from the GIANT consortium, while those for the outcomes were taken from the UK Biobank. The error bars show the 95 confidence interval.